

Accepted for publication in SIAM Journal on Applied Mathematics.

ASYMPTOTIC ANALYSIS OF QUASISTATIC TRANSPORT IN HIGH CONTRAST CONDUCTIVE MEDIA*

LILIANA BORCEA [†]

Abstract. We show that transport in high contrast, conductive media has a discrete behavior. In the asymptotic limit of infinitely high contrast, the effective impedance and the magnetic field in such media are given by discrete min-max variational principles. Furthermore, we show that the transport problem has an asymptotic, resistor-inductor-capacitor network approximation. We use new variational formulations of the effective impedance of the media and we assess the accuracy of the asymptotic approximation by numerical computations.

Key words. high contrast, conductive media, network approximation, effective impedance

AMS subject classifications. 35J25, 35Q60, 86A25, 78A25

1. Introduction. High contrast electromagnetic transport problems arise frequently in geophysical applications. The subsurface electrical conductivity typically has large variations in magnitude (high contrast) because the rock matrix can be insulating in comparison to liquid-filled pores. The conductivity of pore fluids can also vary over several orders of magnitude. For example, the conductivity of water varies over a large range of values with its salinity [3, 23]. Thus, the subsurface conductivity can display very large contrast.

The problem of imaging the subsurface conductivity has been of much interest because of its connection to oil recovery, subsurface flow monitoring, underground contaminant detection, etc. However, most of the available imaging techniques are based on perturbation approximations (Born or Rytov) which assume that the conductivity has small variations in magnitude [2]. These techniques fail in high contrast situations where the inverse problem is highly nonlinear in the unknown conductivity. New techniques that address the issue of nonlinearity of the inverse problem have yet to be found. Such an inversion method was proposed in [8] and has proved to be highly successful in imaging high contrast media when the boundary excitation is time independent. The inversion method in [8] is based on studies of transport properties of high contrast media under static excitation [9, 28]. In [9, 28, 24, 5] it is shown that flow in such media undergoes strong channeling effects that are of crucial importance in the inversion process. In [9] it is shown that static flow through a high contrast medium can be accurately approximated by flow in a discrete resistor network. The authors of [9] also consider time dependent problems, in the low frequency range, for dielectric media. A network approximation consisting of resistors and capacitors for such media is given in [9], although an inversion method based on this approximation is yet to be found.

We consider the problem of transport in high contrast, conductive media in the quasistatic limit (low frequency range). The quasistatic approximation is motivated by the increased interest in imaging subsurface conductivity with low frequency electromagnetic fields [2, 3]. Early research in the imaging field focused on large frequencies because of the wavefield nature of high frequency electromagnetic propagation

*This work was supported by the National Science Foundation under grant number DMS-9627407.

[†]Computational and Applied Mathematics, MS 134, Rice University, 6100 Main Street, Houston, TX 77005-1892 (borcea@caam.rice.edu).

in dielectric media. However, in conductive media these waves are greatly attenuated and cannot penetrate deep enough. Low frequency electromagnetic fields have a much deeper penetration and are therefore preferred for imaging conductive media. We show that quasistatic flow in high contrast conductive media has a discrete behavior and that the effective impedance is given by discrete, min-max variational principles. Furthermore, we show that the transport problem has an asymptotic, resistor-inductor-capacitor network approximation. The analysis is based on new variational principles of saddle-point type. Other variational principles, of Dirichlet type, are also introduced although they are not used in the analysis. Furthermore, we present the results of numerical simulations that assess the accuracy of the asymptotic approximation of transport in high contrast conductive media.

The paper is organized as follows: In section 2 we formulate the equations for quasistatic electromagnetics and introduce a new variational formulation for the effective resistance and inductance of the medium. In section 3 we discuss a particular case of transport in a two component medium consisting of conductive cylinders imbedded in a uniform insulating background. In section 4 we use asymptotic techniques to study some local quasistatic transport problems. We also review the resistor network approximation for static flow in high contrast media. In section 5 we give a detailed analysis of the transport problem in high contrast media. We use new, min-max variational principles and study the existence of a network that approximates transport in high contrast media. In section 6 we present numerical computations that assess the analytical results. Finally, in the appendix, we introduce various, saddle-point or Dirichlet type variational formulations of the effective impedance of conductive media.

2. Formulation of the Quasistatic Electromagnetic Problem and Associated Variational Principles.

2.1. The Quasistatic Equations. We consider Maxwell's equations in a domain Ω that contains no free charges or current sources, with electric and magnetic fields of the form:

$$(1) \quad \begin{aligned} \vec{E}(\mathbf{x}, t) &= \text{real}(\mathbf{E}(\mathbf{x})e^{-i\omega t}), \\ \vec{H}(\mathbf{x}, t) &= \text{real}(\mathbf{H}(\mathbf{x})e^{-i\omega t}), \end{aligned}$$

where ω is the frequency of oscillation. By assuming (1) we restrict our attention to steady state oscillations in a dissipative medium (quasistatic approximation). The complex valued field amplitudes satisfy

$$(2) \quad \begin{aligned} \nabla \times \mathbf{H}(\mathbf{x}) &= \sigma(\mathbf{x})\mathbf{E}(\mathbf{x}) - i\omega\varepsilon(\mathbf{x})\mathbf{E}(\mathbf{x}) \\ \nabla \times \mathbf{E}(\mathbf{x}) &= i\omega\mu(\mathbf{x})\mathbf{H}(\mathbf{x}) \\ \nabla \cdot (\varepsilon(\mathbf{x})\mathbf{E}(\mathbf{x})) &= 0 \\ \nabla \cdot (\mu(\mathbf{x})\mathbf{H}(\mathbf{x})) &= 0, \end{aligned}$$

where σ is the electrical conductivity, ε is the dielectric permittivity and μ is the magnetic permeability. Note that we omit the Maxwell's equation $\nabla \cdot [\mu(\mathbf{x})\mathbf{H}(\mathbf{x})] = 0$ because it is a consequence of the second equation in (2). The Fourier coefficients $\mathbf{E}(\mathbf{x})$ and $\mathbf{H}(\mathbf{x})$ depend on the frequency, as well, but for simplicity we assume ω fixed. The same calculation can be repeated for various frequencies. We assume that the medium is isotropic so σ, ε and μ are scalar functions. For low frequencies ($\omega < 1\text{MHz}$) and conductive media, it is a good approximation [2, 3] to neglect the displacement current and consider the 'pre-Maxwell' equations:

$$\begin{aligned}
 (3) \quad & \nabla \times \mathbf{H}(\mathbf{x}) = \sigma(\mathbf{x})\mathbf{E}(\mathbf{x}) \\
 & \nabla \times \mathbf{E}(\mathbf{x}) = i\omega\mu(\mathbf{x})\mathbf{H}(\mathbf{x}) \\
 & \nabla \cdot (\varepsilon(\mathbf{x})\mathbf{E}(\mathbf{x})) = 0 \\
 & \nabla \cdot (\mu(\mathbf{x})\mathbf{H}(\mathbf{x})) = 0.
 \end{aligned}$$

We consider μ to be the magnetic permeability of the free space ($\mu = \mu_0$) and assume for simplicity that σ is a two dimensional function. All the calculations presented in this paper assume a two dimensional problem but extensions to three dimensions can be done.

We combine the first two equations in (3) to obtain

$$(4) \quad \nabla \times \left[\frac{1}{\sigma(\mathbf{x})} \nabla \times \mathbf{H}(\mathbf{x}) \right] = i\omega\mu\mathbf{H}, \quad \nabla \cdot \mathbf{H}(\mathbf{x}) = 0.$$

We are primarily interested in the application of our analysis to inverse problems, where typical data are measurements of the magnetic field along the boundary [2, 3, 19]. Thus, we consider the Dirichlet boundary conditions

$$(5) \quad \mathbf{H}^{\parallel}(\mathbf{x}) = \psi_R(\mathbf{x}) + i\psi_I(\mathbf{x}), \quad \mathbf{x} \in \partial\Omega,$$

where \mathbf{H}^{\parallel} denotes the component of the magnetic field that is tangential to the boundary. The mathematical problem defined by (4) and (5) has a unique solution (see for instance [13]). The electromagnetic problem (3) can also be written in terms of the electric field, where the boundary conditions consist of the specification of the tangential \mathbf{E} along $\partial\Omega$. This is equivalent to considering equation (4) with the boundary condition $\mathbf{n} \times \mathbf{j}(\mathbf{x}) = \mathbf{I}(\mathbf{x})$, for $\mathbf{x} \in \partial\Omega$, where $\mathbf{j} = \nabla \times \mathbf{H}$ is the current density and \mathbf{n} is the normal at the boundary. Moreover, equation (4) can also be considered in the context of homogenization of periodic media [6], where the excitation consists of the given total current density $\int_{\Omega} \mathbf{j}(\mathbf{x}) d\mathbf{x}$. Motivated by the application of imaging conductive media with low frequency electromagnetic fields, we restrict our analysis to the boundary conditions (5). However, extensions to other boundary conditions can be done. In particular, extensions to the homogenization problem for high contrast, periodic media follow quite easily.

In two-dimensional media and in the transverse magnetic mode, $\mathbf{H} = H(x, y)\mathbf{e}_3$, where \mathbf{e}_3 is the unit vector in the z direction and $\nabla \times \mathbf{H} = -\nabla^{\perp}H$, with $\nabla^{\perp} = \left(-\frac{\partial}{\partial y}, \frac{\partial}{\partial x}\right)$. Thus, (4) reduces to

$$(6) \quad \nabla^{\perp} \cdot [\rho(x, y)\nabla^{\perp}H(x, y)] = -i\omega\mu H(x, y)$$

or, equivalently,

$$(7) \quad \begin{cases} \nabla^{\perp} \cdot [\rho(x, y)\nabla^{\perp}H_R] = \omega\mu H_I \\ \nabla^{\perp} \cdot [\rho(x, y)\nabla^{\perp}H_I] = -\omega\mu H_R, \end{cases}$$

where $\rho = 1/\sigma$ is the local resistance of the medium and $H(x, y) = H_R(x, y) + iH_I(x, y)$ with $H_R, H_I \in \mathbb{R}$. We study the solution of (6) in an arbitrary domain $\Omega \subset \mathbb{R}^2$, with Dirichlet boundary conditions

$$(8) \quad H(\mathbf{x}) = \psi_R(\mathbf{x}) + i\psi_I(\mathbf{x}), \quad \mathbf{x} \in \partial\Omega.$$

We define the current density $\mathbf{j} = \nabla^\perp H$ and we observe that (8) define implicitly the normal flux at the boundary:

$$(9) \quad \Phi(\mathbf{x}) = \mathbf{j}(\mathbf{x}) \cdot \mathbf{n} = \pm \frac{\partial H(\mathbf{x})}{\partial \tau}, \quad \mathbf{x} \in \partial\Omega,$$

where \mathbf{n} is the outward normal to $\partial\Omega$ and $\frac{\partial}{\partial \tau}$ denotes the derivative with respect to the tangential coordinate at the boundary. The plus or minus signs in (9) depend on the orientation of the current \mathbf{j} with respect to the unit normal \mathbf{n} . Thus, the positive sign corresponds to current entering the domain and the negative sign is for the outward flux.

2.2. The High Contrast Model. Our aim in this paper is to study quasistatic transport in media with very high (logarithmic) contrast of σ . Such media could consist, for example, of conductive inclusions imbedded in an insulating matrix. In order to solve (6), (8) we must make assumptions about the shape of the inclusions. In section 3 we consider an example of quasistatic flow in a high contrast medium that consists of a background of conductivity σ_b in which we imbed cylindrical inclusions of conductivity $\sigma_c \gg \sigma_b$. However, such choices cannot be made in the context of inversion so σ should be more general and not depend on particular shapes of inhomogeneities. Therefore, we assume that the high contrast arises in a simple, generic manner as a continuum and propose the model

$$(10) \quad \rho(\mathbf{x}) = \rho_0 e^{\frac{S(\mathbf{x})}{\epsilon^2}},$$

where $S(\mathbf{x})$ is a smooth function defined on Ω , ϵ is a small parameter and ρ_0 is a constant that represents the resistance of a homogeneous reference medium. We assume that the resistance $\rho(\mathbf{x})$ varies everywhere in the domain. Thus, at any point $\mathbf{x} \in \Omega$, $\rho(\mathbf{x})$ has, at some order, at least one nonvanishing derivative (Morse function). Model resistances of the form (10) were used in [28] and [9] for an asymptotic study of transport in high contrast conductive media under static excitation and in [9] for quasistatic transport in dielectrics. Connections with percolation theory are done in [7, 17, 15, 28]. Model resistances of the form (10) were also used in [8] for imaging high contrast conductive media from d.c. boundary measurements.

2.3. Effective Impedance and Variational Principles. In the quasistatic approximation, the wavelength of the electric and magnetic fields is much larger than the characteristic size of the domain Ω so we can use the concept of lumped (effective) impedance of the medium. In this section we derive the expression of the effective impedance and show that its real and imaginary parts have a variational formulation. The new variational principles introduced in this section are of saddle-point type, but other variational formulations are given in the appendix.

We start our derivation by considering Poynting's theorem

$$(11) \quad \int_{\Omega} [\nabla \times \mathbf{H} \cdot \rho \nabla \times \mathbf{H}^* - i\omega\mu \mathbf{H} \cdot \mathbf{H}^*] d\mathbf{x} = -2 \int_{\partial\Omega} \mathbf{S} \cdot \mathbf{n} ds,$$

where \mathbf{n} is the unit normal to $\partial\Omega$ and $\mathbf{S} = \frac{1}{2} \mathbf{E} \times \mathbf{H}^*$ is the Poynting vector averaged over one period of time. The physical interpretation of (11) is as follows: The left hand side in (11) represents the average over a period of time of the rate of change of electromagnetic energy in the domain Ω . The right hand side in (11) gives the flow

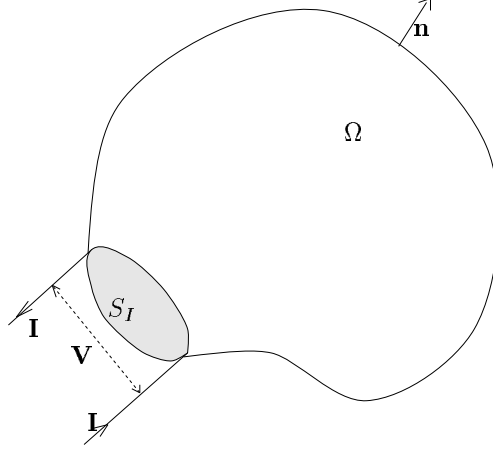


FIG. 1. Energy flows into the domain Ω through surface S_I . The input current and voltage are I and V , respectively.

of energy through the boundary of the domain. If we consider equation (11) over the whole space except Ω , we have

$$(12) \quad \mathbf{I} \cdot \mathbf{V}^* = -2 \int_{S_I} \mathbf{S} \cdot \mathbf{n} ds,$$

where \mathbf{I} and \mathbf{V} are the input current and voltage and S_I is the input surface (see fig. 1). At low frequencies, the radiation escape through $\partial\Omega \setminus S_I$ is negligible [21] so equations (11) and (12) give

$$(13) \quad \mathbf{I} \cdot \mathbf{V}^* = \int_{\Omega} [\nabla \times \mathbf{H} \cdot \rho \nabla \times \mathbf{H}^* - i\omega\mu \mathbf{H} \cdot \mathbf{H}^*] d\mathbf{x}.$$

The linearity of the problem implies that the input voltage is proportional to the input current: $\mathbf{V} = Z\mathbf{I}$, where the coefficient of proportionality is the effective impedance matrix $Z = R - iX$.

The real part of the effective impedance (R) accounts for Ohmic heat loss in the medium and we call it resistance. The imaginary part (X) is called inductive reactance because it gives the magnetic energy stored in Ω . The reactance X is proportional to the inductance L of the medium, where the coefficient of proportionality is the frequency ω . The expressions for R and X are

$$(14) \quad \begin{aligned} \mathbf{I} \cdot R\mathbf{I}^* &= \int_{\Omega} \rho \left(|\nabla \times \mathbf{H}_R|^2 + |\nabla \times \mathbf{H}_I|^2 \right) d\mathbf{x} \\ \mathbf{I} \cdot X\mathbf{I}^* &= \int_{\Omega} \omega\mu \left(|\mathbf{H}_R|^2 + |\mathbf{H}_I|^2 \right) d\mathbf{x}, \end{aligned}$$

where $X = \omega L$ and $\mathbf{H} = \mathbf{H}_R + i\mathbf{H}_I$ satisfies (4) with boundary conditions (5). The input current I is completely determined by the Dirichlet boundary conditions (5). Thus, the normal flux at the boundary is given by

$$(15) \quad \Phi(\mathbf{x}) = \mathbf{n} \cdot \nabla \times \mathbf{H}(\mathbf{x}) = \mathbf{n} \cdot \nabla \times \mathbf{H}^{\parallel}(\mathbf{x}), \text{ for } \mathbf{x} \in \partial\Omega$$

and the input current \mathbf{I} equals the net inward flux, where we assume that the driving is done through a point current source and a point current sink, as shown in figure 1.

Formulation (14) does not lead to a variational principle. However, if we consider instead of (13) the equation

$$(16) \quad - \int_{\partial\Omega} (\mathbf{E} \times \mathbf{H}) \cdot \mathbf{n} ds = \mathbf{I} \cdot Z' \mathbf{I} = \int_{\Omega} [\nabla \times \mathbf{H} \cdot \rho \nabla \times \mathbf{H} - i\omega\mu \mathbf{H} \cdot \mathbf{H}] d\mathbf{x},$$

we obtain

$$(17) \quad \begin{aligned} \mathbf{I} \cdot Z' \mathbf{I} &= \mathbf{I}_R \cdot R' \mathbf{I}_R - \mathbf{I}_I \cdot R' \mathbf{I}_I + 2\mathbf{I}_R \cdot X' \mathbf{I}_I - i [\mathbf{I}_R \cdot X' \mathbf{I}_R - \mathbf{I}_I \cdot X' \mathbf{I}_I - 2\mathbf{I}_R \cdot R' \mathbf{I}_I] \\ &= \int_{\Omega} [\rho (|\nabla \times \mathbf{H}_R|^2 - |\nabla \times \mathbf{H}_I|^2) + 2\omega\mu \mathbf{H}_R \cdot \mathbf{H}_I] d\mathbf{x} - \\ &\quad i \int_{\Omega} [\omega\mu (|\mathbf{H}_R|^2 - |\mathbf{H}_I|^2) - 2\rho \nabla \times \mathbf{H}_R \cdot \nabla \times \mathbf{H}_I] d\mathbf{x}, \end{aligned}$$

where \mathbf{I}_R and \mathbf{I}_I are the real and imaginary parts of the driving current. The ‘generalized’ impedance $Z' = R' - iX'$ is defined by (17) and it is related to the effective impedance $Z = R - iX$ of the medium through

$$(18) \quad \mathbf{I} \cdot Z' \mathbf{I} = - \int_{\partial\Omega} (\mathbf{E} \times \mathbf{H}) \cdot \mathbf{n} ds = \mathbf{I} \cdot Z \mathbf{I}^* - 2i \int_{\partial\Omega} (\mathbf{E} \times \mathbf{H}_I) \cdot \mathbf{n} ds.$$

The integral terms in the right hand side of (18) depend on the tangential flux at the boundary and the imaginary magnetic field (\mathbf{H}_I), tangential to the surface $\partial\Omega$. The generalized impedance Z' has a variational formulation given by the following lemma:

Lemma 2.1 We have the following two variational principles:

$$(19) \quad (\mathbf{I}_R^T \ \mathbf{I}_I^T) \begin{pmatrix} R' & X' \\ X' & -R' \end{pmatrix} \begin{pmatrix} \mathbf{I}_R \\ \mathbf{I}_I \end{pmatrix} =$$

$$\min_{\mathbf{H}_R^{\parallel}|_{\partial\Omega} = \psi_R} \max_{\mathbf{H}_I^{\parallel}|_{\partial\Omega} = \psi_I} \int_{\Omega} [\rho (|\nabla \times \mathbf{H}_R|^2 - |\nabla \times \mathbf{H}_I|^2) + 2\omega\mu \mathbf{H}_R \cdot \mathbf{H}_I] d\mathbf{x}$$

and

$$(20) \quad (\mathbf{I}_R^T \ \mathbf{I}_I^T) \begin{pmatrix} X' & -R' \\ -R' & -X' \end{pmatrix} \begin{pmatrix} \mathbf{I}_R \\ \mathbf{I}_I \end{pmatrix} =$$

$$\min_{\mathbf{H}_R^{\parallel}|_{\partial\Omega} = \psi_R} \max_{\mathbf{H}_I^{\parallel}|_{\partial\Omega} = \psi_I} \int_{\Omega} [\omega\mu (|\mathbf{H}_R|^2 - |\mathbf{H}_I|^2) - 2\rho (\nabla \times \mathbf{H}_R \cdot \nabla \times \mathbf{H}_I)] d\mathbf{x}.$$

Proof: From the first variation of (19) and (20) we obtain

$$(21) \quad \begin{cases} \int_{\Omega} \boldsymbol{\eta} \cdot [\omega\mu \mathbf{H}_I + \nabla \times (\rho \nabla \times \mathbf{H}_R)] d\mathbf{x} = 0 \\ \int_{\Omega} \boldsymbol{\gamma} \cdot [\omega\mu \mathbf{H}_R - \nabla \times (\rho \nabla \times \mathbf{H}_I)] d\mathbf{x} = 0, \end{cases}$$

where $\boldsymbol{\eta}$ and $\boldsymbol{\gamma}$ are arbitrary vector functions that vanish along the boundary $\partial\Omega$ and have continuous second derivatives. Thus, the fields \mathbf{H}_R and \mathbf{H}_I that achieve the min-max in (19) and (20) satisfy

$$(22) \quad \begin{cases} \nabla \times (\rho \nabla \times \mathbf{H}) = i\omega\mu \mathbf{H}, & \mathbf{H} = \mathbf{H}_R + i\mathbf{H}_I, \\ \mathbf{H}_R^{\parallel}(\mathbf{x}) = \psi_R(\mathbf{x}), & \mathbf{H}_I^{\parallel}(\mathbf{x}) = \psi_I(\mathbf{x}) \text{ for } \mathbf{x} \in \partial\Omega. \end{cases}$$

The second variation of (19) gives

$$(23) \quad \int_{\Omega} (\boldsymbol{\eta}^T, \boldsymbol{\gamma}^T) \cdot \begin{pmatrix} \Gamma & \omega\mu\mathbf{I} \\ \omega\mu\mathbf{I} & -\Gamma \end{pmatrix} \begin{pmatrix} \boldsymbol{\eta} \\ \boldsymbol{\gamma} \end{pmatrix},$$

where \mathbf{I} is the identity matrix and $\Gamma = \nabla \times [\rho \nabla \times]$ is a positive, self adjoint operator applied to functions $\boldsymbol{\eta}$ and $\boldsymbol{\gamma}$ that vanish along $\partial\Omega$. The proof of Lemma 2.1 follows immediately from (22) and (23).

We observe that if in (19) and (20) we require that the driving current be real ($\mathbf{I} = \mathbf{I}_R$), we obtain the variational formulation of the real and imaginary parts of Z' . The impedance Z' depends both on the driving current \mathbf{I} and the actual boundary conditions $\boldsymbol{\psi}_R$ and $\boldsymbol{\psi}_I$. The driving current is uniquely determined from the Dirichlet boundary conditions imposed on \mathbf{H}^{\parallel} , as given by (9) and (15). However, the reverse is not true. The normal flux at the boundary determines \mathbf{H}^{\parallel} along $\partial\Omega$ up to an additive constant which is important to know because Z' depends on it. We make the definition of Z' and Z more precise by requiring

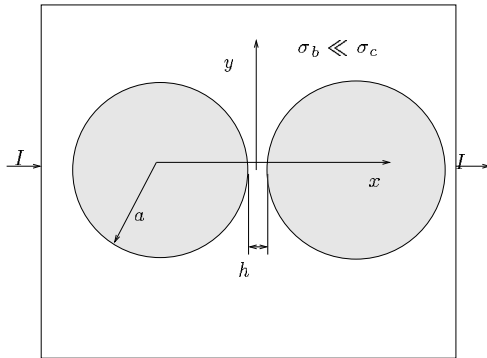
$$(24) \quad \begin{cases} \overline{R}' = \min_{\boldsymbol{\psi}_R} \max_{\boldsymbol{\psi}_I} R'(\boldsymbol{\psi}_R, \boldsymbol{\psi}_I) \\ \overline{X}' = \min_{\boldsymbol{\psi}_R} \max_{\boldsymbol{\psi}_I} X'(\boldsymbol{\psi}_R, \boldsymbol{\psi}_I), \end{cases}$$

where all possible choices of $\boldsymbol{\psi}_R$ and $\boldsymbol{\psi}_I$ give the same input/output current \mathbf{I} . We assume a point current source and sink, so $\boldsymbol{\psi}_R$ and $\boldsymbol{\psi}_I$ are constant along $\partial\Omega$, except near the source and sink, where they change abruptly. The variational principle (24) implies taking the min-max over the constant values of the tangential magnetic field, away from the source or sink. Hence, (24) is just a criterion of fixing the additive constant in the Dirichlet boundary conditions. In section 6 we remove the constraints (24) on the Dirichlet data and we examine the effect of the additive constant on the flow picture and the impedance. The effective impedance $\overline{Z} = \overline{R} - i\overline{X}$ is connected to the generalized impedance $\overline{Z}' = \overline{R}' - i\overline{X}'$ by equation (18). Once the variational problem for \overline{Z}' has been solved, the effective impedance \overline{Z} of the medium can be calculated by evaluating the boundary integrals in (18) that involve the imaginary magnetic field at the boundary and the tangential electric field at $\partial\Omega$.

In this paper we consider equation (4) in an arbitrary domain Ω with Dirichlet boundary conditions (5) and the variational principles:

$$(25) \quad \begin{cases} \mathbf{I} \cdot \overline{R}' \mathbf{I} = \min_{\boldsymbol{\psi}_R} \max_{\boldsymbol{\psi}_I} \min_{\mathbf{H}_R^{\parallel}|_{\partial\Omega}=\boldsymbol{\psi}_R} \max_{\mathbf{H}_I^{\parallel}|_{\partial\Omega}=\boldsymbol{\psi}_I} \left[\int_{\Omega} 2\omega\mu \mathbf{H}_R \cdot \mathbf{H}_I d\mathbf{x} + \right. \\ \left. \int_{\Omega} \rho (|\nabla \times \mathbf{H}_R|^2 - |\nabla \times \mathbf{H}_I|^2) d\mathbf{x} \right] \\ \mathbf{I} \cdot \overline{X}' \mathbf{I} = \min_{\boldsymbol{\psi}_R} \max_{\boldsymbol{\psi}_I} \min_{\mathbf{H}_R^{\parallel}|_{\partial\Omega}=\boldsymbol{\psi}_R} \max_{\mathbf{H}_I^{\parallel}|_{\partial\Omega}=\boldsymbol{\psi}_I} \left[\int_{\Omega} \omega\mu (|\mathbf{H}_R|^2 - |\mathbf{H}_I|^2) - \right. \\ \left. 2\rho \nabla \times \mathbf{H}_R \cdot \nabla \times \mathbf{H}_I d\mathbf{x} \right]. \end{cases}$$

The saddle-point variational principles (25) can be easily extended to the periodic homogenization problem. Indeed, all calculations shown in this section hold for the periodic case. Furthermore, when the driving flow is real, the boundary integral $\int_{\partial\Omega} (\mathbf{E} \times \mathbf{H}_I) \cdot \mathbf{n} ds$ vanishes because of the periodicity of the fields and the impedance

FIG. 2. *High contrast medium with cylindrical inclusions*

Z' is equal to the actual impedance Z (see (18)). The variational principles (25) are different than the variational principles derived by Cherkaev and Gibiansky [10], Fannjiang and Papanicolaou [14, 9] for quasistatic transport in dielectric media, because they involve both the current density $\mathbf{j} = \nabla \times \mathbf{H}$ and the magnetic field \mathbf{H} . The saddle-point structure of (25) is very useful in obtaining lower and upper bounds on the effective parameters R and X . Variational principles of Dirichlet type exist as well, as we show in the appendix. However, such variational principles are not ideal for our analysis because of either the nonlinear dependence on the high contrast resistance ρ or the higher order of the Euler equations. We show in the appendix that the effective impedance has variational formulations in terms of the electric field, as well. Such variational principles are more difficult to use than (25) because the electric field cannot be written in terms of a scalar potential.

3. Quasistatic Transport in a Medium with Conductive Cylindrical Inclusions. In this section we consider a particular example of quasistatic transport in a medium that consists of a uniform background of electrical conductivity σ_b in which we imbed cylindrical inclusions of conductivity $\sigma_c \gg \sigma_b$. We assume that the inclusions are separated from their neighbors by gaps of width h that is much smaller than the radius a of the cylinders. We concentrate on the local problem of flow in the vicinity of two adjacent inclusions shown in figure 2. The static transport properties of such media were studied by J. Keller [24] and later by Batchelor and O'Brien [5]. Keller showed that d.c. current flows through the conductive inclusions and concentrates in the thin gaps in between. The static magnetic field satisfies $\Delta H(x, y) = 0$ inside the inclusions or in the background. The flow in the background is negligible in comparison with the flow in the gap. Hence, the magnetic field (H_b) in the background is approximately a constant. Furthermore, in the gap between the inclusions there is a layer of rapid change of H_b . The asymptotic approximation of the magnetic field in the background is

$$(26) \quad H_b(\mathbf{x}) \approx -\frac{1}{\pi} \arctan \left(\frac{y}{\sqrt{ah}} \right),$$

where we assume a unit input current I . Solution (26) is correct up to an additive constant that, for simplicity, is fixed to zero. The resistance of the medium is given by the resistance of the gap that was computed by Keller [24]: $R_g \approx \frac{1}{\pi\sigma_b} \sqrt{\frac{h}{a}}$.

We return to the quasistatic transport problem and observe that the equation (6)

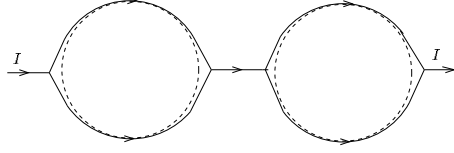


FIG. 3. Flow avoids the conductive regions by concentrating on the surface of the inclusions

reduces to

$$(27) \quad \Delta H = -i\omega\mu\sigma H,$$

where $\sigma = \sigma_b$ in the background and $\sigma = \sigma_c$ inside the inclusions. We assume that $\omega\mu\sigma_b \ll 1$, so the magnetic field in the background is approximately an harmonic function. Thus, the mathematical problem in the background is essentially the same as the static problem and the solution H_b is given by (26). The inclusions are good conductors, so we assume $\omega\mu\sigma_c = \frac{1}{\lambda^2} \gg 1$. The mathematical problem for the magnetic field H_c inside an inclusion is

$$(28) \quad \begin{cases} \lambda^2 \Delta H_c(r, \phi) = -iH_c(r, \phi), & \text{for } r < a \\ H_c(a, \phi) = H_b(a, \phi) \\ \frac{\partial H_c}{\partial r}(a, \phi) = \frac{\sigma_c}{\sigma_b} \frac{\partial H_b}{\partial r}(a, \phi) \gg \frac{\partial H_b}{\partial r}(a, \phi), \end{cases}$$

where (r, ϕ) are polar coordinates with the radius r measured from the center of the cylinder. The solution of (28) is

$$(29) \quad H_c(r, \phi) \approx -\frac{1}{\pi} \arctan\left(\sqrt{\frac{a}{h}} \sin \phi\right) e^{-(1-i)\frac{a-r}{\sqrt{2}\lambda}}.$$

The physical interpretation of (29) is as follows: The magnetic field is expelled from the conductive regions [21, 26, 31, 32] and it penetrates only at the surface of the inclusions, to a depth

$$(30) \quad \lambda = \frac{1}{\sqrt{\omega\mu\sigma_c}} = \text{penetration or skin depth.}$$

Due to the exponential decay of the magnetic field H_c at the surface of the inclusions, we have a strong surface current confined to a thin layer of characteristic width λ ,

$$(31) \quad j_\phi(r, \phi) = \mathbf{j} \cdot \mathbf{e}_\phi \approx \frac{1-i}{\sqrt{2}\pi\lambda} \arctan\left(\sqrt{\frac{a}{h}} \sin \phi\right) e^{-(1-i)\frac{a-r}{\sqrt{2}\lambda}}.$$

We also have a tangential electric field

$$(32) \quad E_\phi(r, \phi) = \mathbf{E}(r, \phi) \cdot \mathbf{e}_\phi \approx \frac{1-i}{\sqrt{2}\pi\lambda\sigma_c} \arctan\left(\sqrt{\frac{a}{h}} \sin \phi\right) e^{-(1-i)\frac{a-r}{\sqrt{2}\lambda}}.$$

Due to the confinement of \mathbf{j} to such a thin layer, we can approximate it by current through a wire of impedance

$$(33) \quad Z_w = R_w - i\omega L_w \approx \frac{(1-i)}{\sqrt{2}} \frac{\pi a}{\lambda\sigma_c}.$$

The impedance per unit length of the wire relates the effective current

$$\int_0^a j_\phi(r, \phi) dr = \frac{1}{\pi} \arctan \left(\sqrt{\frac{a}{h}} \sin \phi \right)$$

to the tangential electric field just outside the wire

$$E_\phi(r, \phi) = \frac{1-i}{\sqrt{2}\pi\lambda\sigma_c} \arctan \left(\sqrt{\frac{a}{h}} \sin \phi \right).$$

Thus, $\frac{dZ_w}{ds} = \frac{1-i}{\sqrt{2}\lambda\sigma_c}$ and integration along the wire (or arclength denoted by s) gives (33). The flow picture is as shown in figure 3. The current concentrates in gaps between cylinders and flows through thin layers at the surface of the conductive inclusions. The discrete behavior of the current density \mathbf{j} suggests that there might be a discrete network approximation for the quasistatic transport problem. We address this issue in section 5, where we use variational principles (25) to study the network approximation.

4. Asymptotic Analysis of Quasistatic Transport in a High Contrast Continuum.

4.1. Review of the Resistor Network Approximation for Static Flow in a High Contrast Continuum. In this section we give a brief review of the asymptotic resistor network approximation for static transport in a high contrast continuum with resistance given by (10). The analysis was done by Kozlov [28], Borcea and Papanicolaou [9]. The results summarized in this section are used in the analysis of quasistatic transport in a high contrast continuum (sections 4.2 and 5).

When the fields are time independent, problem (6) reduces to

$$(34) \quad \begin{cases} \nabla^\perp \cdot (\rho \nabla^\perp H) = 0, & \text{in } \Omega \\ H(\mathbf{x}) = \psi(\mathbf{x}) \in \mathbb{R}, & \mathbf{x} \in \partial\Omega, \end{cases}$$

where $\rho(\mathbf{x})$ is given by (10). The Dirichlet boundary conditions in (34) determine the normal flux at the boundary as explained in section 2.1, equation (9). The static transport equation (34) involves only derivatives of the magnetic field so, the current density $\mathbf{j} = \nabla^\perp H$ and the potential gradient $\nabla\phi = \rho \nabla^\perp H$ in the domain Ω are not affected by arbitrary, additive constants in the Dirichlet boundary conditions. Hence, the results stated in this section are the same for any Dirichlet data $H|_{\partial\Omega} = \psi + C$ (C is an arbitrary constant) that give the same normal flux Φ at the boundary. The input current I is given by the net inward flux $I = \int_{\partial\Omega_{in}} \Phi(\mathbf{x}) d\tau$ and the effective resistance of the medium has the variational formulation

$$(35) \quad I \cdot RI = \min_{\mathbf{j} \cdot \mathbf{n}|_{\partial\Omega} = \Phi} \int_{\Omega} \rho |\nabla^\perp H|^2 d\mathbf{x}.$$

We consider problem (34) with ρ given by (10) for which we seek the solution as a perturbation series $H(\mathbf{x}, \epsilon) = H^{(0)}(\mathbf{x}) + \epsilon^2 H^{(1)}(\mathbf{x}) + \epsilon^4 H^{(2)}(\mathbf{x}) + \dots$. The leading order equation is

$$(36) \quad \nabla^\perp S \cdot \nabla^\perp H^{(0)} = 0$$

and the current density $\mathbf{j} \approx \nabla^\perp H^{(0)}$ is very small in regions of Ω where the gradient $\nabla^\perp S \neq 0$. Around critical points of $\rho(\mathbf{x})$, $\nabla^\perp S$ vanishes and we can have thin layers

of rapid variation of the magnetic field H . Thus, we obtain strong fluxes or current channeling effects. Since the flow seeks the path of minimum resistance (see (35)), the inner layers of flow concentration develop only around minima and saddle points of $\rho(\mathbf{x})$. To state the results, we consider the local problem of flow through a saddle point of $\rho(\mathbf{x})$. In a system of coordinates oriented with the x axis along the direction of the saddle, we have

$$(37) \quad \rho(\mathbf{x}) \approx \rho(\mathbf{x}_S) \exp \left[\frac{k^+(y-y_S)^2}{2\epsilon^2} - \frac{k^-(x-x_S)^2}{2\epsilon^2} \right],$$

where $\mathbf{x}_S = (x_S, y_S)$ is the location of the saddle and k^+ , k^- are the curvatures of the scaled logarithm of ρ at point \mathbf{x}_S . The approximation (37) holds for a small neighborhood of the saddle point: $|x - x_S| \leq \delta$, $|y - y_S| \leq \delta$, where $\delta \rightarrow 0$, such that $\frac{\delta}{\epsilon} \rightarrow \infty$ as $\epsilon \rightarrow 0$. In [28, 9] it is shown that the solution of (34) in the vicinity of \mathbf{x}_S is

$$(38) \quad H(\mathbf{x}) \approx -\frac{1}{2} \operatorname{erf} \left(\sqrt{\frac{k^+}{2}} \frac{(y-y_S)}{\epsilon} \right) + C,$$

where C is an arbitrary constant and we assume a unit flux through the saddle point. The electric potential $\phi(\mathbf{x})$ in the vicinity of \mathbf{x}_S is

$$(39) \quad \phi(\mathbf{x}) \approx -\frac{R_s}{2} \operatorname{erf} \left(\sqrt{\frac{k^-}{2}} \frac{(x-x_S)}{\epsilon} \right) + D,$$

where D is an arbitrary constant. The constant of proportionality R_s is given by

$$(40) \quad R_s = \rho(\mathbf{x}_S) \sqrt{\frac{k^+}{k^-}}$$

and represents the effective resistance of the saddle. Furthermore, the current density given by $\mathbf{j} \approx \frac{1}{\epsilon} \sqrt{\frac{k^+}{2\pi}} e^{-\frac{k^+(y-y_S)^2}{2\epsilon^2}} \mathbf{e}_1$ and the potential gradient approximated by $\nabla\phi \approx \frac{R_s}{\epsilon} \sqrt{\frac{k^-}{2\pi}} e^{-\frac{k^-(x-x_S)^2}{2\epsilon^2}} \mathbf{e}_1$ are localized around the saddle point \mathbf{x}_S and the flow can be approximated by a unit flux through a resistor R_s given by (40).

Around a local minimum $\mathbf{x}_m = (x_m, y_m)$ of the resistance, the shape of function ρ is bowl-like, so there is no preferred direction of flow. The direction of the current density through \mathbf{x}_m is determined by the path of minimum resistance sought by the flow in Ω . The current flows from one minimum to another through saddle points in between. Let us assume that the flow through a local minimum \mathbf{x}_m is along the x direction. In a small neighborhood of \mathbf{x}_m , the resistance is approximately

$$(41) \quad \rho(\mathbf{x}) \approx \rho(\mathbf{x}_m) \exp \left[\frac{p(x-x_m)^2}{2\epsilon^2} + \frac{q(y-y_m)^2}{2\epsilon^2} \right],$$

where p and q are curvatures of the scaled logarithm of ρ at point \mathbf{x}_m . The local expression of the magnetic field is

$$(42) \quad H(\mathbf{x}) \approx \frac{1}{2} \operatorname{erf} \left(\sqrt{\frac{q}{2}} \frac{(y-y_m)}{\epsilon} \right) + C,$$

where C is an arbitrary constant. This gives a current $\mathbf{j} \approx \frac{1}{\epsilon} \sqrt{\frac{q}{2\pi}} e^{-\frac{q(y-y_m)^2}{2\epsilon^2}} \mathbf{e}_1$ that is localized around the minimum \mathbf{x}_m . However, there is no concentration of the potential

gradient at the minimum, so the power dissipated around \mathbf{x}_m is negligible with respect to the heat losses through saddle points of ρ .

The local results given by (38)-(42) are used in conjunction with the variational principle (35) to obtain the resistor network approximation. The analysis is given in [9] and the result is stated by the following lemma:

Lemma 4.1 In the asymptotic limit of infinitely high contrast, static transport in a continuum is approximated by current flow through a discrete resistor network. The nodes of the network are local minima of the resistance and the branches connect two adjacent minima through saddle points. Each branch has a resistance R_s of form (40).

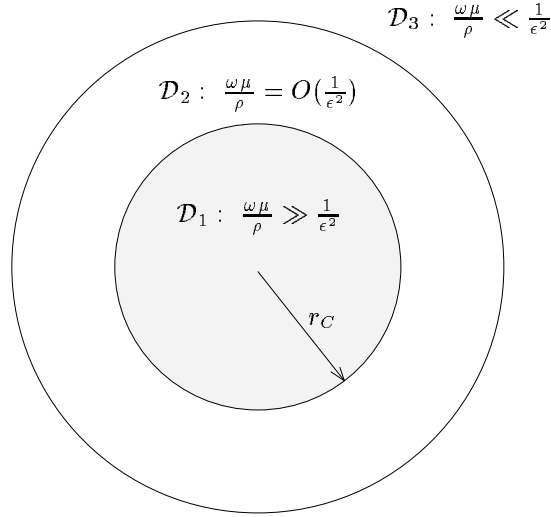


FIG. 4. Domain divided into regions of dominant $\omega\mu$ and dominant ρ

4.2. Local Analysis of Quasistatic Transport Properties of a High Contrast Continuum. We consider the mathematical problem (6), (8) in a high contrast continuum with resistance ρ given by (10). We rewrite the equation as

$$(43) \quad \Delta H + \frac{1}{\epsilon^2} \nabla^\perp S \cdot \nabla^\perp H = -i \frac{\omega\mu}{\rho} H$$

and observe that the behavior of the solution H is dictated by the magnitude of the coefficient $\frac{\omega\mu}{\rho}$ with respect to $\frac{1}{\epsilon^2}$. In regions of dominant resistance ($\frac{\omega\mu}{\rho} \ll \frac{1}{\epsilon^2}$), the mathematical problem is essentially equivalent to the static one (equation (34)) and the magnetic field is calculated as explained in section 4.1. In conductive regions with $\frac{\omega\mu}{\rho} \gg \frac{1}{\epsilon^2}$, the solution of equation (43) is $H \approx 0$. The magnetic field in the strongly conductive regions ($\frac{\omega\mu}{\rho} \gg \frac{1}{\epsilon^2}$) matches the field elsewhere in the flow regime, where the matching domain corresponds to $\frac{\omega\mu}{\rho}$ of order $\frac{1}{\epsilon^2}$. Hence, strongly conductive regions with $\frac{\omega\mu}{\rho} \gg \frac{1}{\epsilon^2}$ are surrounded by layers of exponential decay of the magnetic field.

We begin the asymptotic analysis with a simple situation illustrated in figure 4. We assume that $\frac{\omega\mu}{\rho} \ll \frac{1}{\epsilon^2}$ everywhere in Ω except for a small neighborhood of a local minimum \mathbf{x}_m of ρ . For simplicity, we assume that the shape of the function $\rho(\mathbf{x})$ at the minimum is a circular bowl. We divide the domain Ω into three regions: region

\mathcal{D}_1 , where $\frac{\omega\mu}{\rho} \gg \frac{1}{\epsilon^2}$, region \mathcal{D}_3 with $\frac{\omega\mu}{\rho} \ll \frac{1}{\epsilon^2}$ and the intermediate region \mathcal{D}_2 defined by the condition $\frac{\omega\mu}{\rho} = O(\frac{1}{\epsilon^2})$. Equation (43) indicates that the magnetic field vanishes inside region \mathcal{D}_1 and matches the static field in \mathcal{D}_3 . The matching region is the ring \mathcal{D}_2 . Hence, there is a layer of exponential decay of $H(\mathbf{x})$ near the boundary of the inner region \mathcal{D}_1 . The local expression of the resistance ρ is given by

$$(44) \quad \rho(\mathbf{x}) \approx \rho(\mathbf{x}_m) e^{-\frac{r^2}{2\epsilon^2}},$$

where r is the radial distance measured from the minimum at \mathbf{x}_m . For simplicity, in (44) we assume that the scaled logarithm of the resistance at the minimum has curvatures $p = q = 1$ (see equation (41)). Generalizations to more general shapes of \mathcal{D}_1 and different curvatures p and q are done later in this section.

At the minimum we have $\frac{\omega\mu}{\rho(\mathbf{x}_m)} = \frac{1}{\epsilon^{2+\alpha}} \gg \frac{1}{\epsilon^2}$, where $\alpha = 2 - \frac{\log \frac{\omega\mu}{\rho(\mathbf{x}_m)}}{\log \frac{1}{\epsilon}} > 0$. We define $\mathcal{D}_1 = \{r \mid r < r_C\}$, where $r_C = \epsilon \sqrt{2\alpha \log \frac{1}{\epsilon}} = \frac{\epsilon}{\delta}$, $\delta = \frac{1}{\sqrt{2\alpha \log \frac{1}{\epsilon}}} \rightarrow 0$ as $\epsilon \rightarrow 0$ and $\frac{\omega\mu}{\rho(r_C)} \approx \frac{1}{\epsilon^{2+\alpha}} e^{-\frac{r_C^2}{2\epsilon^2}} = \frac{1}{\epsilon^2}$. In the vicinity of the local minimum \mathbf{x}_m we rewrite the equation (43) in polar coordinates (r, θ) :

$$(45) \quad \frac{\partial^2 H}{\partial r^2} + \frac{1}{r} \frac{\partial H}{\partial r} + \frac{1}{r^2} \frac{\partial^2 H}{\partial \theta^2} + \frac{r}{\epsilon^2} \frac{\partial H}{\partial r} = -\frac{i}{\epsilon^{2+\alpha}} e^{-\frac{r^2}{2\epsilon^2}} H.$$

Since the solution H in the conductive region \mathcal{D}_1 matches the static field $H_s(r, \theta)$ outside, we seek the solution of (45) as $H(r, \theta) = H_s(r, \theta) f(r, \theta)$. The static field $H_s(r, \theta)$ satisfies

$$(46) \quad \frac{\partial^2 H_s}{\partial r^2} + \frac{1}{r} \frac{\partial H_s}{\partial r} + \frac{1}{r^2} \frac{\partial^2 H_s}{\partial \theta^2} + \frac{r}{\epsilon^2} \frac{\partial H_s}{\partial r} = 0,$$

so equation (45) becomes

$$(47) \quad H_s(r, \theta) \left[\frac{\partial^2 f}{\partial r^2} + \frac{1}{r} \frac{\partial f}{\partial r} + \frac{1}{r^2} \frac{\partial^2 f}{\partial \theta^2} + \frac{r}{\epsilon^2} \frac{\partial f}{\partial r} + \frac{i}{\epsilon^{2+\alpha}} e^{-\frac{r^2}{2\epsilon^2}} f \right] + 2\nabla H_s \cdot \nabla f = 0.$$

If we assume an excitation that drives the flow horizontally through the minimum, the static field is given by (see section 4.1)

$$(48) \quad H_s(r, \theta) \approx -\frac{1}{2} \operatorname{erf}\left(\frac{y}{\sqrt{2}\epsilon}\right) + C$$

where $y = r \sin \theta$ and C is a constant that is not arbitrary as in the static case, but determines the flux through the layers of exponential decay of H at the surface of the conductive region \mathcal{D}_1 . Constant C can be found only from the variational principles (25), as we show in section 5. With (48), and scaling $\xi = \frac{r}{\epsilon}$, equation(47) becomes

$$(49) \quad \left[C - \frac{1}{2} \operatorname{erf}\left(\frac{\xi \sin \theta}{\sqrt{2}}\right) \right] \left[\frac{\partial^2 f}{\partial \xi^2} + \frac{1}{\xi} \frac{\partial f}{\partial \xi} + \frac{1}{\xi^2} \frac{\partial^2 f}{\partial \theta^2} + \xi \frac{\partial f}{\partial \xi} + \frac{i}{\epsilon^\alpha} e^{-\frac{\xi^2}{2}} f \right] - \frac{2}{\sqrt{\pi}} \left(\sin \theta \frac{\partial f}{\partial \xi} + \frac{\cos \theta}{\xi} \frac{\partial f}{\partial \theta} \right) e^{-\frac{\xi^2 \sin^2 \theta}{2}} = 0.$$

The layer of exponential decay of $f(\xi, \theta)$ develops near the boundary of \mathcal{D}_1 , given by $\xi = \frac{1}{\delta}$, so we introduce the layer coordinates (η, θ) , where $\eta = \frac{1}{\delta} - \xi$. From

$\xi^2 = (\xi - \frac{1}{\delta} + \frac{1}{\delta})^2 \approx \frac{1}{\delta^2} - 2\frac{\eta}{\delta}$, $\sin \theta e^{-\frac{\xi^2 \sin^2 \theta}{2}} \approx \sin \theta e^{-\frac{\sin^2 \theta}{2\delta^2}}$ and equation (49), we obtain

$$(50) \quad \left[C - \frac{1}{2} \operatorname{erf} \left(\frac{\sin \theta}{\sqrt{2}\delta} \right) \right] \left[\frac{\partial^2 f}{\partial \eta^2} - \delta \frac{\partial f}{\partial \eta} + \delta^2 \frac{\partial^2 f}{\partial \theta^2} - \frac{1}{\delta} \frac{\partial f}{\partial \eta} + i c \frac{\eta}{\delta} f \right] + \frac{2}{\sqrt{\pi}} \left(\sin \theta \frac{\partial f}{\partial \eta} - \delta \cos \theta \frac{\partial f}{\partial \theta} \right) e^{-\frac{\sin^2 \theta}{2\delta^2}} \approx 0.$$

Due to the exponential factor $e^{-\frac{\sin^2 \theta}{2\delta^2}}$ and the inequality $|\sin \theta e^{-\frac{\sin^2 \theta}{2\delta^2}}| \leq \frac{\delta}{\sqrt{e}}$, the last term in the equation (50) is at most of order δ . Hence, at first order, the angular dependence in (50) can be factored out and the leading order approximation of function $f(\cdot)$ is independent on θ . To calculate $f(\cdot)$ from (50), we look for a solution of form $f(\eta) = \exp \left[\frac{S_0(\eta)}{\delta} + S_1(\eta, \theta) + \dots \right]$ which leads to the leading order equation $(S_0'(\eta))^2 - S_0''(\eta) + i\delta^2 e^{\frac{\eta}{\delta}} = 0$, with solution $S_0(\eta) = \frac{\eta}{2} \pm \frac{\delta}{2} \int_0^{\frac{\eta}{\delta}} \sqrt{1 - 4i\delta^2 e^t} dt$. We keep only the decaying solution and the magnetic field is given by

$$(51) \quad H(r, \theta) \approx H_s(r, \theta) \exp \left[\frac{r_C(r_C - r)}{2c^2} - \frac{1}{2} \int_0^{\frac{r_C(r_C - r)}{c^2}} \sqrt{1 - 4i\frac{c^2}{r_C^2} e^t} dt \right].$$

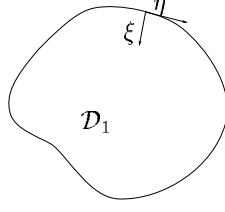
The interpretation of the result (51) is as follows: For $r \geq r_C$ (inside the ring \mathcal{D}_2), the magnetic field matches the static field H_s . Inside region \mathcal{D}_1 , close to the boundary, such that $\frac{c^2}{r_C^2} e^{\frac{r_C(r_C - r)}{c^2}} \ll 1$, the static solution remains valid. However, deeper inside the conductive region \mathcal{D}_1 , the exponential term under the square root in (51) dominates and H decays exponentially fast to zero. Solution (51) depends on the frequency ω through the parameter $r_C(\omega)$ that determines the boundary $\partial\mathcal{D}_1$ of the conductive region. Parameter $r_C(\omega)$ increases with the frequency as shown by

$$(52) \quad r_C(\omega) = c \sqrt{2 \log \left[\frac{c^2 \omega \mu}{\rho(\mathbf{x}_m)} \right]}.$$

Solution (51) is obtained under the assumption that \mathcal{D}_1 is a small vicinity of a local minimum of the resistance, where the curvatures p and q (see equation (41)) of the scaled logarithm of ρ are equal to one. However, the calculation of the magnetic field H that is expelled by conductive regions, can be done for an arbitrary shape of the domain \mathcal{D}_1 . For instance, in a more general situation, we can still have \mathcal{D}_1 as a neighborhood of a local minimum \mathbf{x}_m and curvatures p and q that are not equal to each other. Then, the boundary $\partial\mathcal{D}_1$ is an ellipse and the magnetic field H can be obtained from (51) by using a conformal mapping (see section 6, equation (88)). However, in a general situation, the conductive region \mathcal{D}_1 can include more than a small neighborhood of a local minimum of the resistance, so the boundary $\partial\mathcal{D}_1$ can have an arbitrary shape and conformal mapping cannot be used. We introduce instead a system of coordinates (ξ, η) defined at the boundary $\partial\mathcal{D}_1$, as shown in figure 4.2. The boundary $\partial\mathcal{D}_1$ of the conductive region is defined by the locus of points that give

$$(53) \quad \rho(\mathbf{x}) = c^2 \omega \mu, \text{ for } \mathbf{x} \in \partial\mathcal{D}_1.$$

We look for a solution $H(\xi, \eta) = H_s(\xi, \eta)f(\xi, \eta)$ of equation (43), where $H_s(\cdot)$ is a solution of the static problem (34). In the layer developed near $\partial\mathcal{D}_1$, the function $f(\cdot)$


 FIG. 5. Arbitrary conductive region \mathcal{D}_1 with layer coordinates (ξ, η)

has a very rapid variation in the normal coordinate ξ and a much slower variation in the tangential coordinate η . The local approximation of the resistance is

$$(54) \quad \rho(\xi, \eta) \approx \rho(0, \eta) e^{-\frac{\lambda(\eta)\xi}{\epsilon^2}},$$

where $\rho(0, \eta) = \epsilon^2 \omega \mu$ and $\lambda(\eta) > 0$. Approximation (54) is due to the decrease of the resistance function ρ inside region \mathcal{D}_1 , where $\frac{\omega \mu}{\rho} \gg \frac{1}{\epsilon^2}$. The calculation of $f(\cdot)$ is similar to the one given for the circular region \mathcal{D}_1 and the result is

$$(55) \quad H(\xi, \eta) \approx H_s(\xi, \eta) \exp \left[\frac{\lambda(\eta)\xi}{2\epsilon^2} - \frac{\lambda(\eta)}{2} \int_0^{\frac{\xi}{\epsilon^2}} \sqrt{1 - 4i \frac{\epsilon^2}{\lambda^2(\eta)} e^{\lambda(\eta)t}} dt \right].$$

Solution (55) depends on the frequency ω through parameter $\lambda(\cdot)$. The boundary location and shape of $\partial\mathcal{D}_1$ depend on ω and so does $\lambda(\cdot)$.

4.3. The Effective Impedance. The local analysis of quasistatic transport in a high contrast continuum presented in section 4.2 shows clearly that the magnetic field is expelled from the strongly conductive regions with $\frac{\omega \mu}{\rho} \gg \frac{1}{\epsilon^2}$. Due to this phenomenon, there are thin layers of exponential decay of the magnetic field H and strong surface currents. Thus, we can approximate the transport problem by flow through wires surrounding the conductive regions. The net current through the wires is given by the tangential current density $j_\eta(\xi, \eta) \mathbf{e}_\eta = \frac{\partial H}{\partial \xi}(\xi, \eta) \mathbf{e}_\eta \approx \mathbf{j}(\xi, \eta)$, integrated with respect to ξ across the layers of flow concentration. Since the current is basically tangential to the surface of the conductive region \mathcal{D}_1 , the contour lines of constant magnetic field H are parallel to the boundary $\partial\mathcal{D}_1$. Thus, if in the background of dominant resistance ($\frac{\omega \mu}{\rho} \ll \frac{1}{\epsilon^2}$) the magnetic field is a constant $C + iB$, the net flux through a wire at the boundary $\partial\mathcal{D}_1$ is $I = \int_\infty^0 \frac{\partial H}{\partial t} dt = C + iB$, where $t = \frac{\lambda(\eta)\xi}{\epsilon^2}$, $t \in [0, \infty)$. The surface (wire) impedance, $Z_w = R_w - i\omega L_w$ is obtained from (14), (54) and (55):

$$(56) \quad \begin{aligned} R_w &\approx \omega \mu \int_{\partial\mathcal{D}_1} d\eta \frac{\lambda(\eta)}{4} \int_\infty^0 dt \left| 1 - \sqrt{1 - 4i \frac{\epsilon^2}{\lambda^2} e^t} \right|^2 \left| \exp \left[-\frac{1}{2} \int_0^t \sqrt{1 - 4i \frac{\epsilon^2}{\lambda^2} e^p} dp \right] \right|^2, \\ \omega L_w &\approx \omega \mu \int_{\partial\mathcal{D}_1} d\eta \frac{\epsilon^2}{\lambda(\eta)} \int_\infty^0 dt \left| \exp \left[\frac{1}{2} - \frac{1}{2} \int_0^t \sqrt{1 - 4i \frac{\epsilon^2}{\lambda^2} e^p} dp \right] \right|^2. \end{aligned}$$

Expressions (56) are difficult to calculate in general, unless we evaluate them numerically. However, we observe that both the resistance and inductive reactance are of the form

$$R_w \text{ and } \omega L_w \sim \int_{\partial\mathcal{D}_1} \frac{\epsilon^2 \omega \mu}{\lambda(\eta)} = \int_{\partial\mathcal{D}_1} \frac{\rho(0, \eta)}{\lambda(\eta)},$$

up to some factors of order one. This result is very similar to the surface impedance calculated in section 3 for a medium with conductive cylindrical inclusions. Thus, the surface resistance and inductance are proportional to the resistance at the surface and inverse proportional to the penetration depth $\lambda(\eta)$. The expression of the magnetic field (55) expelled from the conductive region \mathcal{D}_1 is more complicated than solution (29) for cylindrical inclusions, so the definition of the skin depth is more subtle. We define the skin depth λ based on the similarity between the surface impedance calculated from (56) and the impedance given in section 3, equation (33).

5. High Contrast Analysis Based on Variational Principles. In this section we study the global problem of quasistatic transport in a high contrast continuum with resistance (10). The analysis is based on the variational principles (25) for the effective resistance and inductive reactance of the medium. We use the asymptotic results presented in section 4 to choose trial fields in the variational principles and obtain lower and upper bounds on \overline{R} and \overline{X} . Furthermore, we show that the upper and lower bounds on the effective parameters \overline{R} and \overline{Z} match each other as the contrast in the resistance becomes infinitely high, where the matching value is given by a discrete variational principle. Hence, in the asymptotic limit of infinitely high contrast, we can compute the effective impedance of the medium and the magnetic field throughout the domain Ω . We also address the question of approximating quasistatic transport in a high contrast conductive medium by current flow through a discrete network. We show that the flow has a discrete behavior by concentrating around saddle points of the resistance and at the surface of strongly conductive regions. Furthermore, we show that the transport problem admits a network approximation. The branches of the network correspond to the saddle points and the surface of strongly conductive regions, where the current density concentrates. The impedance associated with each branch is not necessarily the resistance of a saddle (see (40)), or the impedance (56) of a wire. We show that the vector of impedances associated with the branches in the network is the solution of a linear, full rank, often underdetermined system of equations, so the network approximation may be nonunique.

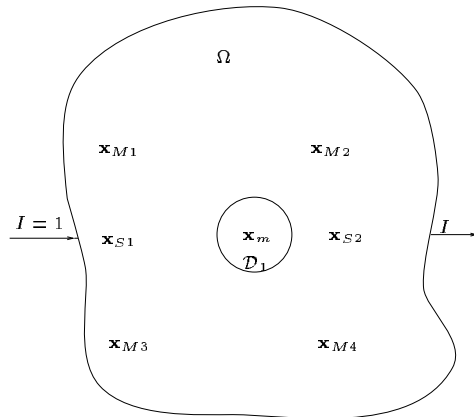


FIG. 6. High contrast continuum with two saddle points \mathbf{x}_{S1} , \mathbf{x}_{S2} and a conductive region \mathcal{D}_1 .

5.1. Example of a Resistor-Inductor Network Approximation of Quasistatic Transport in a High Contrast Continuum. We consider the quasistatic transport problem (6) with Dirichlet boundary conditions (5) in the high contrast

continuum shown in figure 6. The high contrast resistance $\rho(\mathbf{x}) = e^{\frac{S(\mathbf{x})}{\epsilon^2}}$ has two saddle points $\mathbf{x}_{S1} = (x_1, y_1)$ and $\mathbf{x}_{S2} = (x_2, y_2)$, one minimum at \mathbf{x}_m and four maxima \mathbf{x}_{Mi} , $i = 1, \dots, 4$. The analysis is similar for any orientation of the saddle points so, for simplicity, we assume that both saddles are in the horizontal direction. Furthermore, $\frac{\omega\mu}{\rho} \ll \frac{1}{\epsilon^2}$ everywhere in the domain Ω , except in a neighborhood of the minimum \mathbf{x}_m . The external driving force consists of a unit current I , as shown in figure 6. Since there is no imaginary driving current, the imaginary field H_I is constant along the boundary. The real field H_R changes rapidly near the current source and sink, but remains constant elsewhere along the boundary. As we explained in section 2.3, there is an infinite number of Dirichlet data $H_R(\mathbf{x}) = \psi_R(\mathbf{x})$, $H_I(\mathbf{x}) = \psi_I(\mathbf{x})$, for $\mathbf{x} \in \partial\Omega$ that give the same normal current I at the boundary. We restrict attention to the Dirichlet data (5) given by the solution of the saddle point variational principles (25). We use the variational principles (25) to show that quasistatic transport in the high

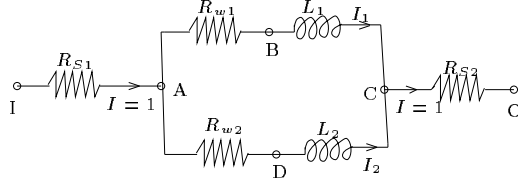


FIG. 7. *Equivalent resistor-inductor network*

contrast continuum shown in figure 6 can be approximated by current flow through the resistor-inductor network shown in figure 7. The significance of the network elements is as follows: The resistors R_{S1} and R_{S2} are due to the flow concentration at saddle points \mathbf{x}_{S1} , \mathbf{x}_{S2} and R_{wi} , L_i $i = 1, 2$ are the resistors and inductors due to the flow at the surface of the conductive region \mathcal{D}_1 .

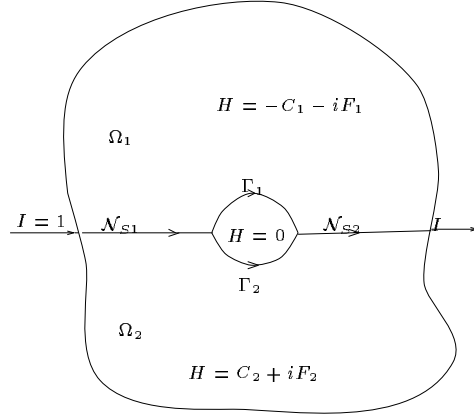
We start the analysis by considering in (25) the following real trial field:

$$(57) \quad H_R(\mathbf{x}) = \begin{cases} -\frac{1}{2} \operatorname{erf} \left(\sqrt{\frac{k_{1,2}^+}{2}} \frac{y - y_{1,2}}{\epsilon} \right) + \frac{C_2 - C_1}{2} & \text{for } \mathbf{x} \in \mathcal{N}_{S1,2} \\ -C_1 h_1 + F_1 g_1 & \mathbf{x} \in \Gamma_1 \\ C_2 h_2 - F_2 g_2 & \mathbf{x} \in \Gamma_2 \\ -C_1 & \mathbf{x} \in \Omega_1 \\ C_2 & \mathbf{x} \in \Omega_2 \\ 0 & \mathbf{x} \in \mathcal{D}_1, \end{cases}$$

where constants C_i and F_i satisfy

$$(58) \quad \begin{cases} C_1 + C_2 = 1 \\ F_1 + F_2 = 0. \end{cases}$$

The trial field H_R given by (57) is chosen according to the asymptotic results obtained in section 4. Thus, inside the conductive region \mathcal{D}_1 , the magnetic field is zero and in the regions of diffuse flow $\Omega_{1,2}$, H is a constant. In the neighborhoods $\mathcal{N}_{S1,2}$ of the saddle points, the magnetic field is given by (38), where $k_{1,2}^+$ are the curvatures, in the direction normal to the flow, of the scaled logarithm of ρ at $\mathbf{x}_{S1,2}$. At the surface of the conductive region \mathcal{D}_1 , the magnetic field decays exponentially fast and a surface current is created. Due to the strong current concentration at the surface,

FIG. 8. Value of the magnetic field H in different regions of Ω

we can approximate the flow by current through the wires $\Gamma_{1,2}$ shown in figure 8. The magnetic field near the wires is given by (see equation (55))

$$H(\mathbf{x}) \approx H_s(\mathbf{x}) [h(\mathbf{x}) + ig(\mathbf{x})],$$

where H_s is the static magnetic field outside region \mathcal{D}_1 and is given by $H_s = -C_1 - iF_1$, for Γ_1 and $H_s = C_2 + iF_2$ for Γ_2 , respectively. Functions $h(\mathbf{x})$ and $g(\mathbf{x})$ are the real and imaginary parts of the exponentially decaying term in (55):

$$\exp \left[\frac{\lambda(\eta)\xi}{2\epsilon^2} - \frac{\lambda(\eta)}{2} \int_0^{\frac{\xi}{\epsilon^2}} \sqrt{1 - 4i \frac{\epsilon^2}{\lambda^2(\eta)} e^{\lambda(\eta)t}} dt \right] = h + ig,$$

where (ξ, η) is the system of coordinates defined along $\Gamma_{1,2}$, with η tangential to the wires.

We use the trial field H_R given by (57) in the variational formulation (25) of the effective resistance and obtain the upper bound

$$\overline{R}' \leq \min_{C_1+C_2=1} \max_{F_1+F_2=0} \mathcal{F}(\mathcal{N}_{S1}) + \mathcal{F}(\mathcal{N}_{S2}) + \mathcal{F}(\mathcal{D}_1) + \mathcal{F}(\Omega_1) + \mathcal{F}(\Omega_2) + \mathcal{F}(\Gamma_1) + \mathcal{F}(\Gamma_2),$$

where each term $\mathcal{F}(\mathcal{D})$ represents a maximization over the imaginary field H_I in the corresponding region denoted by \mathcal{D} . We look first at vicinities of the saddles:

$$\begin{aligned} \mathcal{F}(\mathcal{N}_{S1,2}) &= \max_{I_I=F_1+F_2=0} \int_{\mathcal{N}_{S1,2}} \rho \left[\frac{k_{1,2}^+}{2\pi\epsilon^2} e^{-\frac{k_{1,2}^+(y-y_{1,2})^2}{2\epsilon^2}} - |\nabla^\perp H_I|^2 \right] d\mathbf{x} + \\ (59) \quad & 2\omega\mu \int_{\mathcal{N}_{S1,2}} \left[-\frac{1}{2} \operatorname{erf} \left(\sqrt{\frac{k_{1,2}^+}{2}} \frac{y-y_{1,2}}{\epsilon} \right) + \frac{C_2-C_1}{2} \right] H_I d\mathbf{x}, \end{aligned}$$

where the net imaginary flux I_I is required to be zero. The Euler equation for the imaginary field: $\nabla^\perp (\rho \nabla^\perp H_I) = \omega\mu \left[\frac{1}{2} \operatorname{erf} \left(\sqrt{\frac{k_{1,2}^+}{2}} \frac{y-y_{1,2}}{\epsilon} \right) - \frac{C_2-C_1}{2} \right]$, $\frac{\omega\mu}{\rho} \ll \frac{1}{\epsilon^2}$ has the solution (see section 4)

$$(60) \quad H_I(\mathbf{x}) \approx \text{constant} = -F_1 = F_2, \text{ for } \mathbf{x} \in \mathcal{N}_{S1,2}.$$

Hence, from (60), (59) and the approximation (37) of the resistance near the saddles, we obtain

$$(61) \quad \mathcal{F}(\mathcal{N}_{S_{1,2}}) = R_{S_{1,2}},$$

where R_{S_1} , R_{S_2} are given by (40). In the interior of the conductive region we have

$$(62) \quad \mathcal{F}(\mathcal{D}_1) = -\min_{I_I=0} \rho |\nabla^\perp H_I|^2 d\mathbf{x} \approx 0.$$

In the diffuse regions $\Omega_{1,2}$ there is no net current and

$$\mathcal{F}(\Omega_1) = \max_{I_I=0} \int_{\Omega_1} [\rho |\nabla^\perp H_I|^2 - 2\omega\mu C_1 H_I] d\mathbf{x}.$$

The Euler equation $\nabla^\perp(\rho\nabla^\perp H_I) = \omega\mu C_1$, where $\frac{\omega\mu}{\rho} \ll \frac{1}{\varepsilon^2}$ has the solution $H_I \approx \text{constant} = -F_1$. Hence,

$$(63) \quad \mathcal{F}(\Omega_1) \approx 2\omega\mu C_1 F_1 S_1,$$

where $S_1 = \int_{\Omega_1} d\mathbf{x}$ is the area of region Ω_1 . Similarly,

$$(64) \quad \mathcal{F}(\Omega_2) \approx 2\omega\mu C_2 F_2 S_2.$$

Finally, we look at the transport problem in the vicinity of the wires at the surface of the conductive region \mathcal{D}_1 . We have $\mathcal{F}(\Gamma_1)$ given by

$$\max_{I_I=F_1} \int_{\Gamma_1} \left\{ \rho \left[|-C_1 \nabla^\perp h_1 + F_1 \nabla^\perp g_1|^2 - |\nabla^\perp H_I|^2 \right] + 2\omega\mu(-C_1 h_1 + F_1 g_1) H_I \right\} d\mathbf{x}$$

and the Euler equation $\nabla^\perp(\rho\nabla^\perp H_I) = \omega\mu(C_1 h_1 - F_1 g_1)$ has the solution (see section 4) $H_I(\mathbf{x}) \approx -C_1 g_1(\mathbf{x}) - F_1 h_1(\mathbf{x})$. Hence,

$$(65) \quad \mathcal{F}(\Gamma_1) \approx (C_1^2 - F_1^2) R_{w_1} + 2\omega C_1 F_1 L_{w_1},$$

where R_{w_1} and L_{w_1} are the resistance and inductance of the wire Γ_1 , given by (56). Similarly, for the other wire Γ_2 we have

$$(66) \quad \mathcal{F}(\Gamma_2) \approx (C_2^2 - F_2^2) R_{w_2} + 2\omega C_2 F_2 L_{w_2}.$$

From (5.4)-(5.13) we obtain the upper bound

$$\overline{R}^l \lesssim R_{S_1} + R_{S_2} + \min_{C_1+C_2=1} \max_{F_1+F_2=0} [(C_1^2 - F_1^2) R_{w_1} + 2\omega C_1 F_1 L_1 + (C_2^2 - F_2^2) R_{w_2} + 2\omega C_2 F_2 L_2],$$

where $L_{1,2} = L_{w_{1,2}} + \mu S_{1,2}$ is the inductance of the wires and the regions of diffuse flow. To get a lower bound on \overline{R}^l , we start with the trial imaginary magnetic field

$$(67) \quad H_I(\mathbf{x}) = \begin{cases} -C_1 g_1 - F_1 h_1 & \mathbf{x} \in \Gamma_1 \\ C_2 g_2 + F_2 h_2 & \mathbf{x} \in \Gamma_2 \\ -F_1 & \mathbf{x} \in \Omega_1 \\ F_2 & \mathbf{x} \in \Omega_2 \\ 0 & \mathbf{x} \in \mathcal{D}_1, \end{cases}$$

Element	Net current
$R_{S1,2}$	$I = 1$
$R_{w1} - i\omega L_1$	$I_1 = C_1 + iF_1$
$R_{w2} - i\omega L_2$	$I_2 = C_2 + iF_2$

TABLE 1

Currents through the branches of the resistor-inductor network shown in 7

where $C_1 + C_2 = 1$ and $F_1 + F_2 = 0$. The calculations involved in obtaining the lower bound on \overline{R} are similar to the ones shown above and the result is

$$\overline{R}' \gtrsim R_{S1} + R_{S2} + \min_{C_1+C_2=1} \max_{F_1+F_2=0} [(C_1^2 - F_1^2)R_{w1} + 2\omega C_1 F_1 L_1 + (C_2^2 - F_2^2)R_{w2} + 2\omega C_2 F_2 L_2].$$

Hence, the lower and upper bounds match each other and the effective resistance is given by the discrete, min-max variational principle

$$\overline{R}' \approx R_{S1} + R_{S2} + \min_{C_1+C_2=1} \max_{F_1+F_2=0} [(C_1^2 - F_1^2)R_{w1} + 2\omega C_1 F_1 L_1 + (C_2^2 - F_2^2)R_{w2} + 2\omega C_2 F_2 L_2]. \quad (68)$$

We take the first variation in the discrete saddle point variational principle (68):

$$(69) \quad \begin{cases} \delta C_1 (C_1 R_{w1} + \omega L_1 F_1) + \delta C_2 (C_2 R_{w2} + \omega L_2 F_2) = 0 \\ \delta F_1 (F_1 R_{w1} - \omega L_1 C_1) + \delta F_2 (F_2 R_{w2} - \omega L_2 C_2) = 0, \end{cases}$$

where the perturbation currents satisfy

$$(70) \quad \begin{cases} \delta C_1 + \delta C_2 = 0 \\ \delta F_1 + \delta F_2 = 0. \end{cases}$$

Thus, the constants $C_{1,2}$ and $F_{1,2}$ satisfy the equations

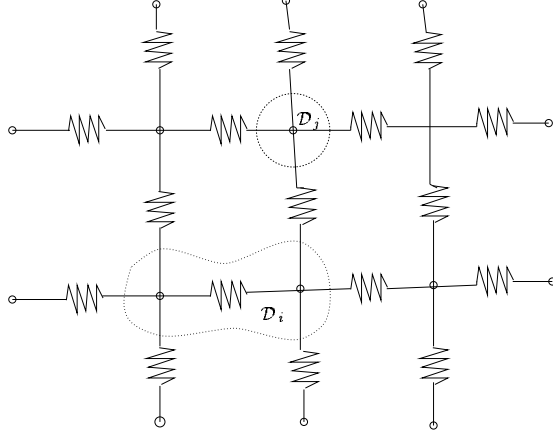
$$(71) \quad \begin{cases} C_1 R_{w1} + \omega L_1 F_1 = C_2 R_{w2} + \omega L_2 F_2 \\ F_1 R_{w1} - \omega L_1 C_1 = F_2 R_{w2} - \omega L_2 C_2 \\ C_1 + C_2 = 1 \\ F_1 + F_2 = 0, \end{cases}$$

which are Kirchhoff's node and loop laws for the resistor-inductor network shown in figure 7. A similar result is obtained for the effective inductive reactance \overline{X}' :

$$\overline{X}' \approx \min_{C_1+C_2=1} \max_{F_1+F_2=0} [(C_1^2 - F_1^2)\omega L_1 - 2C_1 F_1 R_{w1} + (C_2^2 - F_2^2)\omega L_2 - 2C_2 F_2 R_{w2}]. \quad (72)$$

We conclude that quasistatic transport in the high contrast continuum shown in figure 6 can be approximated by current flow through the resistor-inductor network shown in figure 7. The current through each network element is given in table 1, where

$$(73) \quad \begin{cases} C_1 = \frac{R_{w2}(R_{w1}+R_{w2})+\omega L_2(\omega L_1+\omega L_2)}{(\omega L_1+\omega L_2)^2+(R_{w1}+R_{w2})^2} \\ C_2 = 1 - C_1 \\ F_1 = \frac{R_{w2}(\omega L_1+\omega L_2)-\omega L_2(r_1+r_2)}{(\omega L_1+\omega L_2)^2+(R_{w1}+R_{w2})^2} \\ F_2 = -F_1. \end{cases}$$


 FIG. 9. *Modification of the static resistor network*

The generalized impedance \overline{Z}' is given by the impedance of the circuit shown in figure 7:

$$(74) \quad \overline{Z}' = R_{S1} + R_{S2} + \left[\frac{1}{R_{w1} - i\omega L_1} + \frac{1}{R_{w2} - i\omega L_2} \right]^{-1}.$$

Finally, we compute the effective impedance \overline{Z} of the medium from equations (18) and (74):

$$(75) \quad \begin{cases} \overline{R} = \overline{R}' + 2 \int_{\partial\Omega} H_I \rho \frac{\partial H_I}{\partial n} ds \\ \overline{X} = \overline{X}' + 2 \int_{\partial\Omega} H_I \rho \frac{\partial H_R}{\partial n} ds. \end{cases}$$

The imaginary field H_I is a constant along the boundary and from (6) we have

$$(76) \quad \int_{\partial\Omega} \rho \frac{\partial H}{\partial n} ds = -i\omega\mu \int_{\Omega} H d\mathbf{x},$$

where

$$(77) \quad \int_{\Omega} H d\mathbf{x} \approx -(C_1 + iF_1)S_1 + (C_2 + iF_2)S_2.$$

Hence, from (68), (75)-(77) we obtain the effective resistance of the medium

$$\overline{R} \approx R_{S1} + R_{S2} + (C_1^2 - F_1^2)R_{w1} + 2\omega C_1 F_1 L_{w1} + (C_2^2 - F_2^2)R_{w2} + 2\omega C_2 F_2 L_{w2},$$

where the terms $2\omega C_i F_i \mu S_i$, $i = 1, 2$ due to the regions $\Omega_{1,2}$ of diffuse flow have been subtracted. Thus, as definition (14) shows, heat dissipation occurs only in the part of the domain with significant current density: at saddle points and along the wires on the surface of the conductive regions. However, the regions $\Omega_{1,2}$ of diffuse flow are important in determining the magnitude of the currents flowing through each network element.

5.2. The Effective Quasistatic Impedance of a High Contrast Continuum. The resistor-inductor network approximation obtained in section 5.1 corresponds to a high contrast continuum with the particular geometry shown in figure 6. In this section we consider more general situations and explore the validity of the network approximation. We show that quasistatic transport in a high contrast continuum with resistance (10) can be approximated by flow through a discrete network. The branches of the network correspond to the saddle points of ρ in regions with $\frac{\omega\mu}{\rho} \ll \frac{1}{\epsilon^2}$ and to thin layers (wires) at the surface of strongly conductive regions, where $\frac{\omega\mu}{\rho} \gg \frac{1}{\epsilon^2}$. However, the impedance associated with each branch may not be simply the resistance of the saddle points or the impedance of the wires given by equations (40) and (56). Instead, we show that the vector of impedances satisfies a linear, full rank, usually underdetermined system.

In general, to obtain the asymptotic network approximation we first identify its topology. We do so by drawing first the static resistor network (see Lemma 4.1), where the nodes of the network are minima of ρ and the branches connect two adjacent minima through a saddle point. We illustrate such a resistor network in figure 9. Next, we identify the strongly conductive regions in Ω , where the condition $\frac{\omega\mu}{\rho} \gg \frac{1}{\epsilon^2}$ is satisfied. We draw two such regions \mathcal{D}_i and \mathcal{D}_j in figure 9. The analysis presented in section 4 shows that, inside the conductive regions \mathcal{D}_i , the magnetic field vanishes. Furthermore, outside \mathcal{D}_i , the magnetic field is approximately equal to a solution of the static problem. Hence, near saddle points, H changes abruptly across the direction of the current through the saddles and is constant elsewhere in the flow regime. This leads to flow channeling at the saddle points and the approximation by current through a resistor R_S given by (40). The net current through each saddle point is given by the difference between the magnetic field above and below the flow line. The conductive regions \mathcal{D}_i expel the magnetic field, so there are strong surface currents around them. Due to the small depth of the surface layers, we approximate the surface currents by currents through wires of impedance per unit length $\frac{dZ_w(\eta)}{d\eta}$ given by (56), where η is the coordinate tangent to the surface of \mathcal{D}_i . The net current through the wires at the surface of \mathcal{D}_i is given by the magnitude of the static magnetic field outside \mathcal{D}_i . The topology of the network is clear now. The branches of the network are given by either the paths through saddle points (if $\frac{\omega\mu}{\rho} \ll \frac{1}{\epsilon^2}$) or by the wires around the strongly conductive regions, where $\frac{\omega\mu}{\rho} \gg \frac{1}{\epsilon^2}$. The nodes of the network are either minima of ρ that are connected through a saddle point, or the points of intersection between the contour of the static resistor network and the conductive regions \mathcal{D}_i .

Let us assume that there are N_C regions \mathcal{D}_i , $i = 1, \dots, N_C$, where the resistance ρ is small enough so $\frac{\omega\mu}{\rho} \gg \frac{1}{\epsilon^2}$ is satisfied. The rest of the domain is divided into N_D regions Ω_i , $i = 1, \dots, N_D$ of diffuse flow, where the division is done by the flow path, as explained in the example shown in section 5.1. Due to the thin regions of

flow concentration, we have $\Omega \approx \left(\bigcup_{i=1}^{N_D} \Omega_i \right) \cup \left(\bigcup_{i=1}^{N_C} \mathcal{D}_i \right)$. Suppose that out of N branches,

N_S correspond to saddle points and the rest $N_w = N - N_S$ are given by wires. To determine the magnetic field H and the effective impedance, we use the variational principles (25). The analysis is similar to the one illustrated in section 5.1. Thus, we start with a trial field H_R that is suggested by the asymptotic analysis given in section 4 and we obtain an upper bound on \overline{R} and \overline{X} . To get lower bounds on the bulk parameters \overline{R} and \overline{X} , we choose an appropriate imaginary trial field H_I . The bounds match each other when the contrast in ρ tends to infinity and the matching

values are given by discrete min-max variational principles in terms of the constant field H in the regions of diffuse flow Ω_i . We use the notation

$$(78) \quad H(\mathbf{x}) \approx C_j + iF_j$$

for points \mathbf{x} in the regions of diffuse flow, Ω_j , $j = 1, \dots, N_D$. The currents through the saddle points are given by

$$(79) \quad I_{S_j} = -(C_l + iF_l) + (C_k + iF_k), \quad j = 1, \dots, N_S,$$

where the indices l and k correspond to the diffuse regions $\Omega_{l,k}$ right above and below the flow line through the saddle j . The currents through the wires are

$$(80) \quad I_{w_j} = C_l + iF_l, \quad j = 1, \dots, N_w,$$

where the index l corresponds to the region of diffuse flow Ω_l in the immediate vicinity of the wire j .

The effective resistance and inductive reactance are given by

$$(81) \quad \left\{ \begin{array}{l} \overline{R}' \approx \min_{C_j} \max_{F_j} \left[\sum_{j=1}^{N_S} (I_{S_j}^{(R)2} - I_{S_j}^{(I)2}) R_{S_j} + 2 \sum_{j=1}^{N_D} C_j F_j \omega \mu S_j + \right. \\ \left. \sum_{j=1}^{N_w} [(I_{w_j}^{(R)2} - I_{w_j}^{(I)2}) R_{w_j} + 2 I_{w_j}^{(I)} I_{w_j}^{(R)} \omega L_{w_j}] \right] \\ \overline{X}' \approx \min_{C_j} \max_{F_j} \left[\sum_{j=1}^{N_D} (C_j^2 - F_j^2) \omega \mu S_j - 2 \sum_{j=1}^{N_S} I_{S_j}^{(R)} I_{S_j}^{(I)} R_{S_j} + \right. \\ \left. \sum_{j=1}^{N_w} [(I_{w_j}^{(R)2} - I_{w_j}^{(I)2}) \omega L_{w_j} - 2 I_{w_j}^{(I)} I_{w_j}^{(R)} R_{w_j}] \right] \end{array} \right.$$

where $S_j = \int_{\Omega_j} d\mathbf{x}$, $j = 1, \dots, N_D$ and the superindices (R) and (I) denote the real and imaginary parts of the currents I_{S_j} and I_{w_j} . There are also two constraints imposed on the constants C_i and F_i that establish the driving current. From the first variation of (81) and the two constraint equations we obtain a full rank, linear system of $2N_D$ equations with $2N_D$ unknowns C_i , and F_i , $i = 1, \dots, N_D$ which determines uniquely the asymptotic approximation of the magnetic field H in the domain Ω . Furthermore, once C_i and F_i , $i = 1, \dots, N_D$ are known, we calculate the effective impedance $\overline{Z}' = \overline{R}' - i\overline{X}'$ from (81).

Thus, the variational principles are very powerful tools for calculating the asymptotic approximation of the magnetic field in media with high contrast. The discrete variational formulation of the effective impedance and the flow concentration in Ω leads us to the question of existence of an asymptotic network that approximates the flow through the medium. If there is such a network, the currents through each branch must coincide with the currents calculated above from the variational principles. Furthermore, the network must have the same equivalent impedance \overline{Z}' as the one given by (81). In the network, to each branch j we associate an impedance z_j , where $j = 1, \dots, N$. Then, if a network exists, the algebraic sums of the potential drops in each closed loop must be zero, (Kirchhoff's loop law) and

$$(82) \quad \overline{Z}' = \sum_{j=1}^N I_j^2 z_j.$$

There are no other constraints because the currents I_j , $j = 1, N$ computed from the variational principles satisfy Kirchhoff's node laws. To write explicitly the system of equations satisfied by z_j , we introduce the spanning network matrix A . The rows of A correspond to loops in the circuit and the columns denote the branches, where each branch is assigned a direction. We define the matrix A as follows:

$$(83) \quad A_{j,k} = \begin{cases} +1 & \text{if branch } k \in \text{loop } j, \text{ and is oriented clockwise} \\ -1 & \text{if branch } k \in \text{loop } j, \text{ and is oriented counterclockwise} \\ 0 & \text{if branch } k \notin \text{loop } j. \end{cases}$$

The matrix A is in general singular, so we define a reduced matrix \tilde{A} where we keep only the linearly independent rows. These rows correspond to all the independent loops in the circuit. Let us assume that there are p independent loops in the circuit, where $p + 1$ must be smaller than the number N of branches in the circuit. Furthermore, we assume that all currents I_j , $j = 1, \dots, N$ are nonzero. If some currents are zero, the corresponding branches play no part in the network and are completely eliminated. With the help of the matrix \tilde{A} , we now write the set of independent Kirchhoff's loop laws as

$$(84) \quad \tilde{A}\mathcal{I} = \mathbf{0},$$

where \mathcal{I} is the diagonal matrix $\mathcal{I} = \text{diag}(I_1, I_2, \dots, I_N)$. Then, we have

$$(85) \quad B\mathbf{z} = \begin{pmatrix} \mathbf{c}^T \\ \tilde{A} \end{pmatrix} \mathcal{I}\mathbf{z} = \begin{pmatrix} \overline{\mathcal{Z}}^T \\ \mathbf{0} \end{pmatrix},$$

where \mathbf{z} is the vector of unknown impedances and $\mathbf{c}^T = (I_1, I_2, \dots, I_N)$. The matrix $\tilde{A} \in \mathbb{R}^{p \times N}$, where $p \leq N - 1$ has p independent columns, and since $I_i \neq 0, \forall i = 1, \dots, N$, the matrix $\tilde{A}\mathcal{I}$ has p independent columns, as well. Hence, the matrix B has full rank and the linear system of equations (85) has a solution. Furthermore, in general, (85) has fewer equations than unknowns, so the solution can be nonunique. This means that we can choose $N - p$ impedances, where the condition

$$(86) \quad \text{real}(z_i) \geq 0, \quad i = 1, \dots, N$$

must be satisfied.

We now return to the example studied in section 5.1, where we found the equivalent resistor-inductor network shown in figure 7. In this example, the matrix A is

$$\begin{pmatrix} 0 & 1 & -1 & 0 \\ 0 & 1 & -1 & 0 \end{pmatrix}$$

where we have two loops: IABCODAI and ABCD. Since the first loop contains the second, the matrix A has rank one, and

$$\tilde{A} = (0, 1, -1, 0).$$

Furthermore,

$$B = \begin{pmatrix} 1 & I_1^2 & I_2^2 & 1 \\ 0 & I_1 & -I_2 & 0 \end{pmatrix}$$

has two independent columns. It is a matter of simple algebra to check that one of the solutions of (85) gives the network shown in figure 7.

We conclude this section with a note concerning the Dirichlet boundary conditions (8) imposed on the magnetic field. We concentrated attention on the Dirichlet boundary conditions that achieve the min-max in the variational principle (24). For arbitrary Dirichlet boundary conditions, the analysis remains the same, except that in the variational principles, there are additional equality constraints imposed on the constant fields in the diffuse regions that contain a piece of the boundary. Due to these constraints, the magnitude of the currents through the branches of the network varies with the Dirichlet boundary conditions. However, the current density maintains its discrete behavior and follows the same path. Furthermore, the magnetic field H in the domain Ω and the effective impedance Z' of the medium are determined by discrete, min-max variational principles similar to (81), but with fixed, assigned values of the constant fields C_j and D_j at the boundary $\partial\Omega$. Hence, the calculation of \bar{Z} and the asymptotic approximation of $H(x, y)$ in Ω remains essentially unchanged for any Dirichlet boundary conditions. Furthermore, the network approximation developed in this section applies to arbitrary Dirichlet data. However, the currents and the impedance associated with the branches of the network change with the boundary conditions. The network can consist of resistors, inductors and capacitors. The presence of capacitors in the network approximation is crucial because it allows for rotational currents (eddies) that can develop for some Dirichlet boundary conditions. An example that illustrates this last statement is considered in section 6.

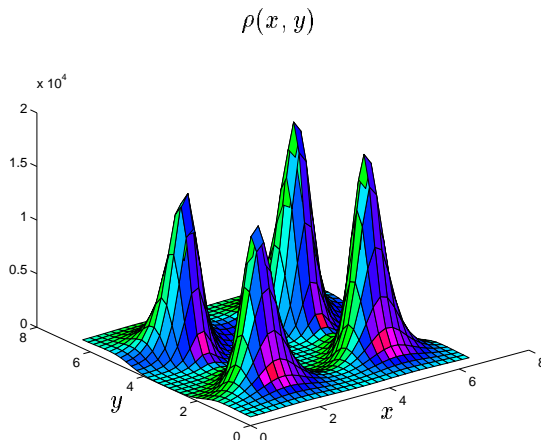
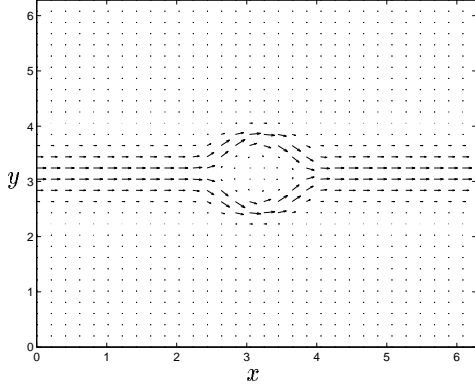
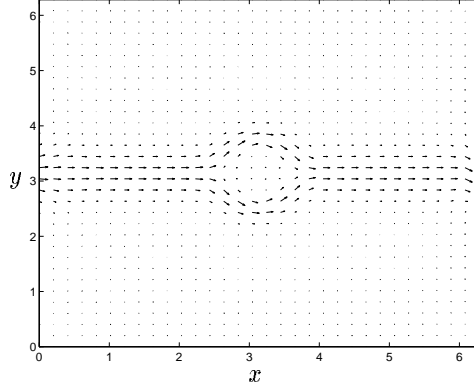
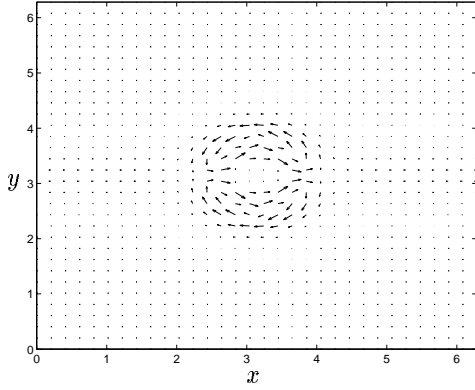
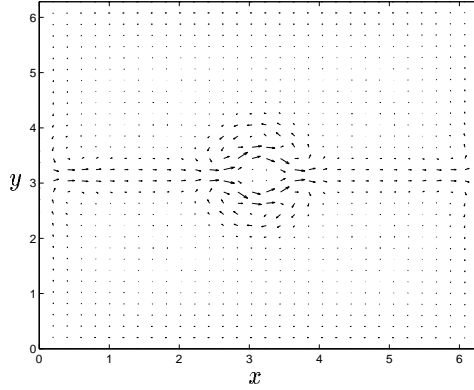


FIG. 10. Resistance of high contrast medium that has the network approximation shown in fig. 7

6. Numerical Computations. In this section, we present the results of some numerical experiments that illustrate the analysis carried out in the previous sections. We solve the complex equation (6) with Dirichlet boundary conditions (5) in a square domain $\Omega = [0, 2\pi] \times [0, 2\pi]$. We use a second order finite difference method and a uniform discretization of the domain Ω . In all the numerical calculations presented in this section we use a mesh with 64 grid points in each direction. We also tested the convergence by halving the mesh spacing and comparing the solutions. We check first the asymptotic expression (55) of the magnetic field at the surface of a conductive region, where $\frac{\omega\mu}{\rho} \gg \frac{1}{\epsilon^2}$. The first numerical experiment is also designed to test the resistor-inductor network approximation given in section 5.1. We use the resistance function $\rho(\mathbf{x})$ shown in figure 10, where the geometry is similar to the one shown in 6.

FIG. 11. *Real, asymptotic flow*FIG. 12. *Real, numeric flow*FIG. 13. *Imaginary, asymptotic flow*FIG. 14. *Imaginary, numeric flow*

We have two horizontal saddle points $\mathbf{x}_{S1} = (\frac{\pi}{2}, \pi)$, $\mathbf{x}_{S2} = (\frac{3\pi}{2}, \pi)$ and one minimum $\mathbf{x}_m = (\pi, \pi)$ in between. The contrast is 4.548×10^4 , $\epsilon^2 = 0.15$ and $\omega\mu = 150$. At the minimum, $\frac{\omega\mu}{\rho(\mathbf{x}_m)} = \frac{1}{\epsilon^2 + \alpha}$, where $\alpha = 3.856$. The curvatures of the scaled logarithm of ρ at the minimum are $p = 1.1193$ and $q = 1.257$ (see equation (41)). At the saddle points $\mathbf{x}_{S1,2}$ we have $\rho(\mathbf{x}_{S1}) = 333$, $\rho(\mathbf{x}_{S2}) = 663$ and the curvatures are $k_1^+ = 0.86$, $k_1^- = 0.94$, $k_2^+ = 0.8$ and $k_2^- = 1$, respectively. Due to the symmetry with respect to the axis $y = \pi$, equations (73) give $C_1 = C_2 = \pi$ and $D_1 = D_2 = 0$, where we assume an input current $I = 2\pi$. In the numerical experiment we consider a current source at $\mathbf{x} = (0, \pi)$ and a sink at $\mathbf{x} = (2\pi, \pi)$. We approximate point sources by Gaussian pulses and prescribe the boundary condition

$$(87) \quad H(x, y) = -\pi \operatorname{erf} \left(\frac{y - \pi}{0.1\sqrt{2}} \right), \text{ for } (x, y) \in \partial\Omega.$$

The frequency ω is chosen such that $\omega\mu = 150$ dominates the resistance only around the minimum \mathbf{x}_m . Due to the different curvatures of ρ at the minimum, the boundary of the conductive region \mathcal{D}_1 is an ellipse. Thus, for the purpose of comparison between the numerical and asymptotic magnetic field near \mathcal{D}_1 , we use the magnetic field derived from (51) through a conformal map that transforms the polar coordinates

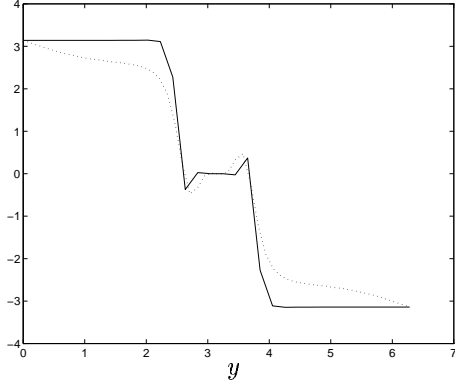


FIG. 15. Real magnetic field along the vertical line $x = \pi$. The full line corresponds to the asymptotic solution and the dotted line to the numeric one

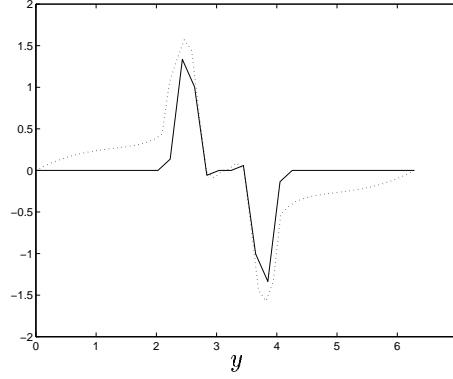


FIG. 16. Imaginary magnetic field along the vertical line $x = \pi$. The full line corresponds to the asymptotic solution and the dotted line to the numeric one

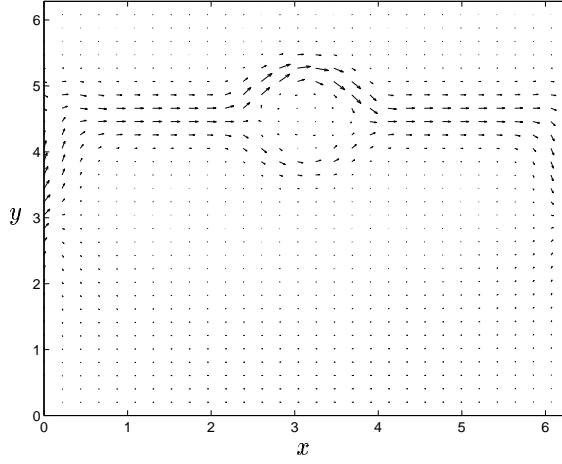


FIG. 17. Real current flow. Stronger current through the branch with lower impedance

$r = \sqrt{(x - x_m)^2 + (y - y_m)^2}$, and θ into the coordinates ξ and α defined by

$$\xi = \frac{r}{2} \left[1 + \left(1 - 8 \frac{b^2}{r^2} \cos(2\theta) + 16 \frac{b^4}{r^4} \right)^{\frac{1}{2}} + 2 \left(1 - 8 \frac{b^2}{r^2} \cos(2\theta) + 16 \frac{b^4}{r^4} \right)^{\frac{1}{4}} \cos(\theta - \beta) \right]^{\frac{1}{2}},$$

$$\alpha = \arctan \left[\tan \theta \frac{1 + \left(1 - 8 \frac{b^2}{r^2} \cos(2\theta) + 16 \frac{b^4}{r^4} \right)^{\frac{1}{4}} \frac{\sin \beta}{\sin \theta}}{1 + \left(1 - 8 \frac{b^2}{r^2} \cos(2\theta) + 16 \frac{b^4}{r^4} \right)^{\frac{1}{4}} \frac{\cos \beta}{\cos \theta}} \right],$$

where $\beta = \frac{1}{2} \arctan \left[\frac{\sin(2\theta)}{\cos(2\theta) - 4b^2} \right]$. The focal distance of the ellipse is given by $2b = r_C \sqrt{\frac{q-p}{p}}$, where r_C is defined in (52). The magnetic field is given by

$$(88) \quad H(\xi, \alpha) \approx H_s(\xi, \alpha) \exp \left[\frac{qr_E(r_E - \xi)}{2c^2} - \frac{q}{2} \int_0^{\frac{r_E(r_E - \xi)}{c^2}} \sqrt{1 - 4i \frac{c^2}{q^2 r_E^2} e^{qt}} dt \right],$$

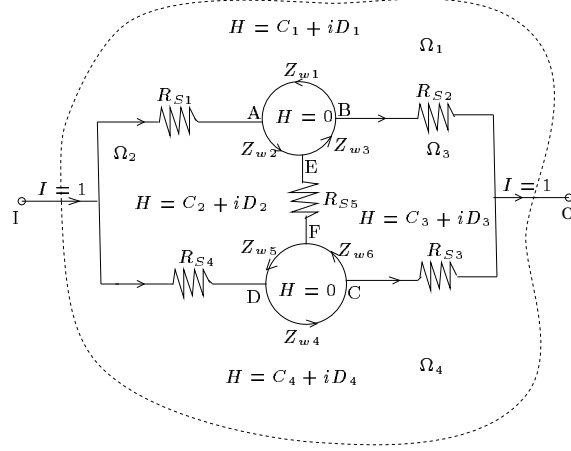


FIG. 18. *Magnetic field distribution over the computational domain Ω shown with dotted line. The static network and surface currents around conductive regions are drawn in full line.*

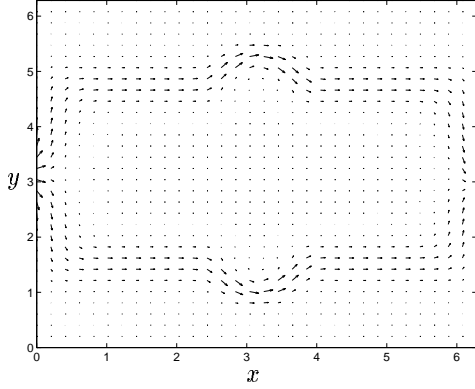


FIG. 19. *Real current flow*

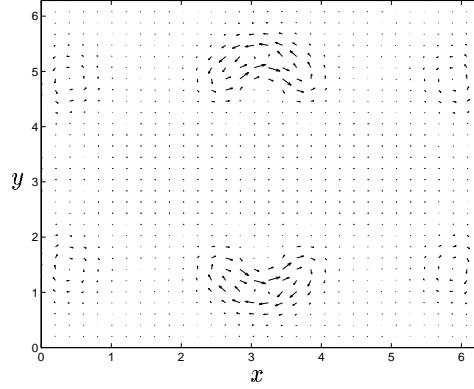


FIG. 20. *Imaginary current flow*

where $r_E = \frac{r_C}{2\sqrt{k}}(1 + \sqrt{k})$. The asymptotic and numeric flow fields are shown in figures 11-14. We observe that the results are very similar and they show clearly the flow concentration through the network sketched in figure 7. Furthermore, the picture of the imaginary flow shows that near the strongly conductive region \mathcal{D}_1 there is imaginary current. However, the current changes direction through both the top and bottom layers and the net imaginary flux is zero. We test the asymptotic expression derived in section 4 for the magnetic field expelled by \mathcal{D}_1 , by comparing the real and imaginary parts of H along the vertical line $x = \pi$. We show the results in figures 15 and 16, where the asymptotic field is drawn with full line. The comparison is quite good near the conductive region \mathcal{D}_1 and slightly worse near the boundary. This is due to the lower term corrections that become important near $\partial\Omega$, where ρ is almost flat (see figure 10). In the asymptotic approximation, we assume high contrast everywhere in the flow regime, so the error seen in figures 15 and 16 is to be expected. The resistance of the saddles is computed from (40): $R_{S1} = 318.5147$ and $R_{S2} = 593.0052$. The resistance and inductive reactance of the wires are computed by evaluating numerically the integrals in (56). We use Simpson's rule for the interval $t \in [0, 100]$, with 500 grid points. The results are $R_{w1} = R_{w2} = 39.076$

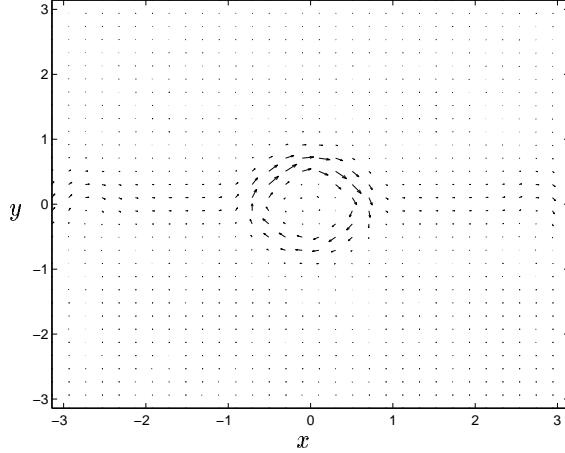


FIG. 21. Real current flow for arbitrary Dirichlet boundary conditions.

and $\omega L_{w1} = \omega L_{w2} = 39.324$. The background inductive reactance is estimated to $\omega\mu(S_1 + S_2) = 1110.3305$. Thus, the asymptotic approximation of the impedance is $\bar{Z} \approx 931.0579 - i1129.87$. The numerical value of the impedance is $\bar{Z} = 957.1239 - i1076.93$. Hence the asymptotic resistance is accurate within 2.8% and the error in the inductance is 4.92%.

In the next numerical experiment we test the effect of the distributed inductive reactance on the currents in the branches of the network shown in figure 7. We keep all the parameters the same as before, but we move the critical points upwards, from $y = \pi$ to $y = 1.4\pi$. The current source and sink are kept in the same position, but the value of H along $\partial\Omega$ is changed according to (73). The real current flow is shown in figure 17 and, as predicted, the upper branch of smaller inductance has the strongest net flux. From (73) we obtain that

$$\begin{cases} C_1 + iD_1 \approx 4.40 - i0.017 \\ C_2 + iD_2 \approx 1.88 + i0.017. \end{cases}$$

Thus, in the upper and lower branches we have the net real currents of 4.40 and 1.88, respectively. The numerical fluxes are 4.23 and 1.69, respectively.

In the third numerical experiment, we consider the more complex network problem shown in figure 18. There are four horizontal saddle points: $\mathbf{x}_{S1} = (\frac{\pi}{2}, \frac{3\pi}{2})$, $\mathbf{x}_{S2} = (\frac{3\pi}{2}, \frac{3\pi}{2})$, $\mathbf{x}_{S3} = (\frac{3\pi}{2}, \frac{\pi}{2})$, $\mathbf{x}_{S4} = (\frac{\pi}{2}, \frac{\pi}{2})$ and a vertical one $\mathbf{x}_{S5} = (\pi, \pi)$. We also have two conductive regions $\mathcal{D}_{1,2}$ surrounding the minima $\mathbf{x}_{m1} = (\pi, \frac{3\pi}{2})$ and $\mathbf{x}_{m2} = (\pi, \frac{\pi}{2})$. The resistance at the horizontal saddle points is given by $\rho(\mathbf{x}_{Si}) = 385$, $i = 1, \dots, 4$ and $\rho(\mathbf{x}_{S5}) = 123.456$. At the minima, $\rho(\mathbf{x}_{mi}) = 0.37$ and $\omega\mu = 100$. The contrast in ρ is 5.4×10^4 and $\epsilon^2 = 0.15$. The symmetry of the problem leads to the solution (see figure 18)

$$\begin{cases} C_1 = -\pi \\ C_2 = C_3 = 0 \\ C_4 = \pi \\ D_1 = D_2 = D_3 = D_4 = 0, \end{cases}$$

where we assume the same boundary conditions (87). The real and imaginary flows are shown in figures 19 and 20 and it is clear that the network consists of the horizontal

saddles and the wires of impedance $Z_{w1} - i\omega\mu S_1$ and $Z_{w4} - i\omega\mu S_4$. The rest of the wires, as well as the vertical saddle have no current through them, so they do not have any contribution to the network.

In the final experiment presented in this section, we illustrate the effect of the Dirichlet boundary conditions on the network approximation. This was discussed at the end of section 5.2. We return to the first experiment presented in this section, where we keep all the parameters the same but change the boundary conditions (87) to

$$H(x, y) = -3.3 - \pi \operatorname{erf}\left(\frac{y - \pi}{0.1\sqrt{2}}\right), \text{ for } (x, y) \in \partial\Omega.$$

The real flow is shown in figure 21 and, as explained in section 5.2, it is different from the flow through the network shown in figure 12. Furthermore, we observe that in the lower branch we have countergradient flow which leads to a rotational current around the conductive region surrounding the minimum at $\mathbf{x}_m = (\pi, \pi)$. The currents through the wires are $I_{w1} = 6.4416$ and $I_{w2} = -0.1584$, so from Kirchhoff's loop law we obtain $6.4416Z_{w1} = -0.1584Z_{w2}$. Since the rotational current is real, the impedance associated with each branch in the loop around the minimum is strictly imaginary, where one wire is inductive and the other is capacitive. Thus, in general, the asymptotic network is not restricted to resistors and inductors. The presence of capacitors is important because it allows for rotational currents (eddies) to form.

7. Summary and Conclusions. We have shown both analytically and numerically that quasistatic transport in a high contrast continuum has a discrete behavior. The flow concentrates at saddle points of the resistance and around very conductive regions that expel the magnetic field. Due to this discrete behavior, the effective impedance of high contrast media is approximated by discrete, min-max variational principles in terms of the constant values of the magnetic field in the regions of diffuse flow. Hence, the magnetic field in a high contrast continuum is given by the solution of a linear system of equations. Furthermore, we show that quasistatic transport in high contrast conductive media can be approximated by flow through a resistor-inductor-capacitor network. The topology of the network is a modification of the static one, where strongly conductive regions are taken out and replaced by wires along their boundaries. The problem of associating to each branch in the network an impedance is a little more subtle. One has to solve a linear, full rank system of equations. In general, this system is underdetermined so there may be more than one network that give the same effective impedance and have the same currents through their branches.

We have also demonstrated the effect of the frequency ω on the transport properties of high contrast conductive media. We have shown that, for low frequencies, transport is very similar to the static one. The flow follows the path given by the static resistor network, although the magnitude of the currents is slightly different. As the frequency increases, the currents through the branches of the static network change even more. For even higher frequencies, there are regions in the domain that expel the magnetic field and the topology of the network changes. The quasistatic transport problem in conductive media admits various variational formulations, as we show in the appendix. We use in the analysis min-max variational formulations of the effective impedance of the medium. We have restricted attention to two dimensional problems but extensions to more dimensions can be done. The results obtained in this paper are not limited to a high contrast continuum, but they apply to isotropic materials with discontinuous, high contrast resistance, as well. Such an example is

the high contrast medium with cylindrical inclusions considered in section 3.

Appendix: Variational Principles for Quasistatic Transport in Conductive Media. In this section we introduce some variational formulations for the problem of quasistatic transport in conductive media. We derive variational principles of saddle-point and Dirichlet type and show their connection with the variational principles (25) introduced in section 2.3. Recall from section 2.1, equations (3), that

$$(89) \quad \begin{aligned} \rho \nabla \times \mathbf{H}_R &= \mathbf{E}_R \\ \rho \nabla \times \mathbf{H}_I &= \mathbf{E}_I \\ \nabla \times \mathbf{E}_R &= -\omega \mu \mathbf{H}_I \\ \nabla \times \mathbf{E}_I &= \omega \mu \mathbf{H}_R \\ \nabla \cdot \mathbf{H}_R &= \nabla \cdot \mathbf{H}_I = 0. \end{aligned}$$

We define the electric and magnetic fields as

$$(90) \quad \begin{cases} \mathbf{H} = \nabla \times \mathbf{A}, & \mathbf{A} = \mathbf{A}_R + i\mathbf{A}_I \\ \mathbf{E} = \nabla \phi + i\omega \mu \mathbf{A}, & \phi = \phi_R + i\phi_I, \end{cases}$$

where \mathbf{A} is the vector, magnetic potential and ϕ can be viewed as a scalar, electric potential. With definitions (90), equations (89) can be rewritten as

$$(91) \quad \begin{cases} \nabla \phi_R = \rho \nabla \times \nabla \times \mathbf{A}_R + \omega \mu \mathbf{A}_I \\ \nabla \phi_I = \rho \nabla \times \nabla \times \mathbf{A}_I - \omega \mu \mathbf{A}_R. \end{cases}$$

The system of equations (91) is the basis of our derivation of various variational principles of saddle-point and Dirichlet type. These variational principles are shown to be interrelated via Legendre transformations of convex or saddle functionals, taken over the real or imaginary potentials \mathbf{A} and ϕ , respectively. Furthermore, the Legendre transformations are shown to be equivalent to excluding pairs of potentials in the system of equations (91).

Let us start by excluding the scalar potentials ϕ_R and ϕ_I in (91). We take the curl in the equations (91) and obtain the system

$$(92) \quad \begin{cases} \nabla \times \rho \nabla \times \nabla \times \mathbf{A}_R + \omega \mu \nabla \times \mathbf{A}_I = 0 \\ \nabla \times \rho \nabla \times \nabla \times \mathbf{A}_I - \omega \mu \nabla \times \mathbf{A}_R = 0, \end{cases}$$

that is equivalent to the system of Euler equations (22) corresponding to the variational principle

$$(93) \quad R' = \min_{\mathbf{H}_R^{\parallel}|_{\partial\Omega} = \boldsymbol{\psi}_R} \max_{\mathbf{H}_I^{\parallel}|_{\partial\Omega} = \boldsymbol{\psi}_I} U_{AA},$$

where the superindex \parallel denotes the tangential components at the boundary surface and

$$(94) \quad U_{AA} = \int_{\Omega} [\rho (|\nabla \times \mathbf{H}_R|^2 - |\nabla \times \mathbf{H}_I|^2) + 2\omega \mu \mathbf{H}_R \cdot \mathbf{H}_I] d\mathbf{x}.$$

With $\mathbf{H}_R = \nabla \times \mathbf{A}_R$ we obtain

$$(95) \quad U_{AA} = \int_{\Omega} g(\mathbf{A}_R, \nabla \times \mathbf{H}_I) d\mathbf{x} + 2\omega \mu \int_{\partial\Omega} (\mathbf{A}_R \times \boldsymbol{\psi}_I) \cdot \mathbf{n} ds,$$

where

$$(96) \quad g(\mathbf{A}_R, \nabla \times \mathbf{H}_I) = \rho |\nabla \times \nabla \times \mathbf{A}_R|^2 - \rho |\nabla \times \mathbf{H}_I|^2 + 2\omega\mu \mathbf{A}_R \cdot \nabla \times \mathbf{H}_I.$$

We take the Legendre transformation of the saddle functional $g(\cdot, \cdot)$, over the imaginary current $\mathbf{j}_I = \nabla \times \mathbf{H}_I$:

$$(97) \quad \tilde{g}(\mathbf{A}_R, \mathbf{G}) = \max_{\mathbf{j}_I} [2\mathbf{j}_I \cdot \mathbf{G} + g(\mathbf{A}_R, \mathbf{j}_I)],$$

where $\tilde{g}(\cdot, \cdot)$ is conjugate about the second variable to the saddle-type function $g(\cdot, \cdot)$. The field \mathbf{G} that is conjugate to the imaginary current \mathbf{j}_I is given by

$$(98) \quad \mathbf{G} = \rho \mathbf{j}_I - \omega\mu \mathbf{A}_R = \nabla \phi_I$$

and the conjugate functional is

$$(99) \quad \tilde{g}(\mathbf{A}_R, \mathbf{G}) = \rho |\nabla \times \nabla \times \mathbf{A}_R|^2 + \frac{(\omega\mu)^2}{\rho} \mathbf{A}_R \cdot \mathbf{A}_R + \frac{1}{\rho} \mathbf{G} \cdot \mathbf{G} + 2 \frac{\omega\mu}{\rho} \mathbf{A}_R \cdot \mathbf{G}.$$

The Legendre transformation (97) is equivalent to eliminating the pair of potentials \mathbf{A}_I and ϕ_R and rewriting the system (91) as

$$(100) \quad \begin{cases} \nabla \cdot \left[\frac{1}{\rho} \nabla \phi_I + \frac{\omega\mu}{\rho} \mathbf{A}_R \right] = 0 \\ \nabla \times \nabla \times \rho \nabla \times \nabla \times \mathbf{A}_R + \frac{(\omega\mu)^2}{\rho} \mathbf{A}_R + \frac{\omega\mu}{\rho} \nabla \phi_I = 0, \end{cases}$$

with boundary conditions

$$(101) \quad \begin{cases} \mathbf{A}_R^\parallel = \gamma_R, \quad (\nabla \times \mathbf{A}_R)^\parallel = \psi_R, \quad \text{where } \gamma_R \text{ and } \psi_R \text{ are given along } \partial\Omega \\ \mathbf{j}_I \cdot \mathbf{n} = \frac{1}{\rho} (\nabla \phi_I + \omega\mu \mathbf{A}_R) \cdot \mathbf{n} = 0, \quad \text{for } \mathbf{x} \in \partial\Omega. \end{cases}$$

We have the following variational formulation of the resistance of the medium:

$$(102) \quad R = \min_{\mathbf{A}_R} \min_{\nabla \phi_I} U_{A\phi},$$

where

$$U_{A\phi} = \int_{\Omega} \left[\rho |\nabla \times \nabla \times \mathbf{A}_R|^2 + \frac{(\omega\mu)^2}{\rho} \mathbf{A}_R \cdot \mathbf{A}_R + \frac{1}{\rho} \nabla \phi_I \cdot \nabla \phi_I + 2 \frac{\omega\mu}{\rho} \mathbf{A}_R \cdot \nabla \phi_I \right] d\mathbf{x}.$$

The proof of the variational principle (102) is very similar to the proof of Lemma 2.1. We consider the first variation in (102):

$$(103) \quad \begin{aligned} \delta U_{A\phi} = & \int_{\Omega} \delta \mathbf{A}_R \cdot \left[\nabla \times \nabla \times \rho \nabla \times \nabla \times \mathbf{A}_R + \frac{(\omega\mu)^2}{\rho} \mathbf{A}_R + \frac{\omega\mu}{\rho} \nabla \phi_I \right] d\mathbf{x} - \\ & \int_{\Omega} \delta \phi_I \nabla \cdot \left(\frac{1}{\rho} \nabla \phi_I + \frac{\omega\mu}{\rho} \mathbf{A}_R \right) d\mathbf{x} + \int_{\partial\Omega} (\delta \mathbf{A}_R \times \nabla \times \rho \nabla \times \nabla \times \mathbf{A}_R) \cdot \mathbf{n} ds + \\ & \int_{\partial\Omega} (\nabla \delta \mathbf{A}_R \times \rho \nabla \times \nabla \times \mathbf{A}_R) \cdot \mathbf{n} ds + \int_{\partial\Omega} \delta \phi_I \left[\frac{1}{\rho} (\nabla \phi_I + \omega\mu \mathbf{A}_R) \right] \cdot \mathbf{n} ds = 0. \end{aligned}$$

The boundary conditions imposed on the tangential components of \mathbf{A}_R and $\nabla \times \mathbf{A}_R$ require that, for $\mathbf{x} \in \partial\Omega$, $\delta \mathbf{A}_R^\parallel = 0$ and $(\nabla \times \delta \mathbf{A}_R)^\parallel = 0$. Hence, the first two boundary integrals in (103) vanish and we obtain

$$(104) \quad \begin{aligned} & \int_{\Omega} \delta \mathbf{A}_R \cdot \left[\nabla \times \nabla \times \rho \nabla \times \nabla \times \mathbf{A}_R + \frac{(\omega\mu)^2}{\rho} \mathbf{A}_R + \frac{\omega\mu}{\rho} \nabla \phi_I \right] d\mathbf{x} - \\ & \int_{\Omega} \delta \phi_I \nabla \cdot \left(\frac{1}{\rho} \nabla \phi_I + \frac{\omega\mu}{\rho} \mathbf{A}_R \right) d\mathbf{x} + \int_{\partial\Omega} \delta \phi_I \left[\frac{1}{\rho} (\nabla \phi_I + \omega\mu \mathbf{A}_R) \right] \cdot \mathbf{n} ds = 0, \end{aligned}$$

for any variations $\delta \mathbf{A}_R$ and $\delta \phi_I$. Hence, the Euler equations that the minimizers satisfy are exactly (100). The minimal structure of the variational principle follows from the second variation

$$(105) \quad \delta^2 U_{A\phi} = \int_{\Omega} \rho |\nabla \times \nabla \times \delta \mathbf{A}_R|^2 + \frac{1}{\rho} |\omega \mu \delta \mathbf{A}_R + \nabla \delta \phi_I|^2 d\mathbf{x} > 0.$$

Furthermore, at the minimum, $U_{A\phi}$ equals the effective resistance of the medium (see definition (14)).

We consider next, instead of (97), a Legendre transformation over the real current

$$(106) \quad \max_{\mathbf{j}_R} [2\nabla \phi_R \cdot \mathbf{j}_R - f(\mathbf{j}_R, \mathbf{A}_I)],$$

where $f(\cdot, \cdot)$ is defined by $f(\mathbf{j}_R, \mathbf{A}_I) = \rho |\mathbf{j}_R|^2 - \rho |\nabla \times \nabla \times \mathbf{A}_I|^2 + 2\omega \mu \mathbf{A}_I \cdot \mathbf{j}_R$. The Legendre transformation (106) is equivalent to eliminating the pair of potentials \mathbf{A}_R and ϕ_I in (91). Thus, we obtain the Euler equations

$$(107) \quad \begin{cases} \nabla \cdot \left[\frac{1}{\rho} \nabla \phi_R - \frac{\omega \mu}{\rho} \mathbf{A}_I \right] = 0 \\ \nabla \times \nabla \times \rho \nabla \times \nabla \times \mathbf{A}_I + \frac{(\omega \mu)^2}{\rho} \mathbf{A}_I - \frac{\omega \mu}{\rho} \nabla \phi_R = 0, \end{cases}$$

with boundary conditions

$$(108) \quad \begin{cases} \mathbf{A}_I^{\parallel} = \gamma_I, (\nabla \times \mathbf{A}_I)^{\parallel} = \psi_I, \text{ where } \gamma_I \text{ and } \psi_I \text{ are given along } \partial\Omega \\ \mathbf{j}_R \cdot \mathbf{n} = \frac{1}{\rho} (\nabla \phi_R - \omega \mu \mathbf{A}_I) \cdot \mathbf{n} = I_R, \text{ for } \mathbf{x} \in \partial\Omega. \end{cases}$$

We have the following minimum variational principle

$$(109) \quad \min_{\nabla \phi_R} \min_{\mathbf{A}_I} U_{\phi A},$$

where

$$(110) \quad U_{\phi A} = \int_{\Omega} \left[\rho |\nabla \times \nabla \times \mathbf{A}_I|^2 + \frac{(\omega \mu)^2}{\rho} |\mathbf{A}_I|^2 + \frac{1}{\rho} |\nabla \phi_R|^2 - 2 \frac{\omega \mu}{\rho} \mathbf{A}_I \cdot \nabla \phi_R \right] d\mathbf{x} - \int_{\partial\Omega} \phi_R I_R ds.$$

At the minimum, we calculate the effective resistance of the medium as

$$R = U_{\phi A} + \int_{\partial\Omega} \phi_R I_R ds.$$

Finally, we derive a variational principle in terms of the scalar potentials ϕ_R and ϕ_I . Simple calculations show that by eliminating \mathbf{A}_R and \mathbf{A}_I in (91) we obtain

$$(111) \quad \begin{cases} \nabla \cdot \left(\frac{1}{\rho} \nabla \phi_R \right) - \omega \mu \nabla \cdot \left(\frac{1}{\rho} \Gamma^{-1} \frac{1}{\rho} \nabla \phi_I \right) + (\omega \mu)^3 \nabla \cdot \left[\frac{1}{\rho} \Gamma^{-1} \frac{1}{\rho} \left(\Gamma \rho \Gamma + \frac{(\omega \mu)^2}{\rho} I \right)^{-1} \frac{1}{\rho} \nabla \phi_I \right] = 0 \\ \nabla \cdot \left(\frac{1}{\rho} \nabla \phi_I \right) + \omega \mu \nabla \cdot \left(\frac{1}{\rho} \Gamma^{-1} \frac{1}{\rho} \nabla \phi_R \right) - (\omega \mu)^3 \nabla \cdot \left[\frac{1}{\rho} \Gamma^{-1} \frac{1}{\rho} \left(\Gamma \rho \Gamma + \frac{(\omega \mu)^2}{\rho} I \right)^{-1} \frac{1}{\rho} \nabla \phi_R \right] = 0, \end{cases}$$

where I is the identity, the operator $\Gamma = \nabla \times \nabla \times$ is symmetric and positive definite and we assume, for simplicity, Dirichlet boundary conditions

$$(112) \quad \begin{cases} \phi_R = \alpha_R \\ \phi_I = \alpha_I, \text{ for } \mathbf{x} \in \partial\Omega. \end{cases}$$

Then, we have the following saddle-point variational principle

$$(113) \quad M = \min_{\phi_R} \max_{\phi_I} U_{\phi\phi},$$

where

$$(114) \quad U_{\phi\phi} = \int_{\Omega} \left[\frac{|\nabla\phi_R|^2}{\rho} - \frac{|\nabla\phi_I|^2}{\rho} - 2\omega\mu\nabla\phi_R \cdot \frac{1}{\rho}\Gamma^{-1}\frac{1}{\rho}\nabla\phi_I + \right. \\ \left. 2(\omega\mu)^3\nabla\phi_R \cdot \frac{1}{\rho}\Gamma^{-1}\frac{1}{\rho}(\Gamma\rho\Gamma + \frac{(\omega\mu)^2}{\rho}I)^{-1}\frac{1}{\rho}\nabla\phi_I \right] d\mathbf{x}.$$

Furthermore, at the saddle point, the effective resistance is given by

$$R^I = M + \int_{\partial\Omega} (\boldsymbol{\gamma}_I \times \boldsymbol{\psi}_R + \boldsymbol{\gamma}_R \times \boldsymbol{\psi}_I) \cdot \mathbf{n} ds,$$

where $\boldsymbol{\gamma} = \boldsymbol{\gamma}_R + i\boldsymbol{\gamma}_I$ and $\boldsymbol{\psi} = \boldsymbol{\psi}_R + i\boldsymbol{\psi}_I$ denote the components of \mathbf{A} and \mathbf{H} that are tangent to the boundary surface $\partial\Omega$.

The above variational principles are interrelated via Legendre transformations that are equivalent to excluding various pairs of potentials in the system of equations (91). The relations between the variational principles are explained by the following: The min-max variational principle

$$(115) \quad \min_{\mathbf{H}_R} \max_{\mathbf{H}_I} U_{AA}$$

is transformed through a Legendre transformation over \mathbf{A}_I (see (97)) into

$$(116) \quad \min_{\mathbf{A}_R} \min_{\phi_I} U_{A\phi}.$$

Next, we consider a Legendre transformation over \mathbf{A}_R or, equivalently, eliminate \mathbf{A}_R and \mathbf{A}_I in (91) to obtain another min-max principle, that is equivalent to (113):

$$(117) \quad \min_{\phi_I} \max_{\phi_R} (-U_{\phi\phi}).$$

Finally, we take a Legendre transformation over ϕ_I and (117) becomes

$$(118) \quad \max_{\phi_R} \max_{\mathbf{A}_I} (-U_{\phi A}),$$

which is equivalent to (110).

All the above variational formulations give the effective resistance of the medium. Next, we derive a minimum variational formulation of the effective inductive reactance. We start with the min-max variational principle

$$X' = \min_{\mathbf{H}_R|_{\partial\Omega}=\boldsymbol{\psi}_R} \max_{\mathbf{H}_I|_{\partial\Omega}=\boldsymbol{\psi}_I} \int_{\partial\Omega} [\omega\mu(|\mathbf{H}_R|^2 - |\mathbf{H}_I|^2) - 2\rho\nabla \times \mathbf{H}_R \cdot \nabla \times \mathbf{H}_I] d\mathbf{x},$$

which we rewrite as

$$(119) \quad X' = \min_{\mathbf{D}|_{\partial\Omega}=\boldsymbol{\psi}_R-\boldsymbol{\psi}_I} \max_{\mathbf{B}|_{\partial\Omega}=\boldsymbol{\psi}_R+\boldsymbol{\psi}_I} \int_{\partial\Omega} \left[\frac{\rho}{2} |\nabla \times \mathbf{D}|^2 - \frac{\rho}{2} |\nabla \times \mathbf{B}|^2 + \omega\mu \mathbf{B} \cdot \mathbf{D} \right] d\mathbf{x},$$

where the fields

$$(120) \quad \begin{cases} \mathbf{B} = \mathbf{H}_R + \mathbf{H}_I \\ \mathbf{D} = \mathbf{H}_R - \mathbf{H}_I \end{cases}$$

satisfy the Euler equations

$$(121) \quad \begin{cases} \nabla \times (\rho \nabla \times \mathbf{B}) = \omega \mu \mathbf{D} \\ \nabla \times (\rho \nabla \times \mathbf{D}) = -\omega \mu \mathbf{B}. \end{cases}$$

Clearly, both \mathbf{B} and \mathbf{D} are divergence free fields, so we write

$$(122) \quad \mathbf{D} = \nabla \times \mathbf{C} = \nabla \times (\mathbf{A}_R - \mathbf{A}_I).$$

Then, (119) becomes

$$(123) \quad X' + \omega \mu \int_{\partial\Omega} [(\boldsymbol{\psi}_R + \boldsymbol{\psi}_I) \times (\boldsymbol{\gamma}_R - \boldsymbol{\gamma}_I)] ds = \min_{\mathbf{C}} \max_{\nabla \times \mathbf{B}} \int_{\Omega} h(\mathbf{C}, \nabla \times \mathbf{B}) d\mathbf{x},$$

where $h(\mathbf{C}, \nabla \times \mathbf{B}) = \frac{\rho}{2} |\nabla \times \nabla \times \mathbf{C}|^2 - \frac{\rho}{2} |\nabla \times \mathbf{B}|^2 + \omega \mu \mathbf{C} \cdot \nabla \times \mathbf{B}$ and the boundary conditions imposed on the potential \mathbf{C} are

$$(124) \quad \begin{cases} \mathbf{C}^{\parallel} = \boldsymbol{\gamma}_R - \boldsymbol{\gamma}_I \\ (\nabla \times \mathbf{C})^{\parallel} = \boldsymbol{\psi}_R - \boldsymbol{\psi}_I, \text{ for } \mathbf{x} \in \partial\Omega. \end{cases}$$

We take the Legendre transformation of the saddle functional $h(\cdot, \cdot)$, over the current $\nabla \times \mathbf{B}$ and obtain

$$(125) \quad \tilde{h}(\mathbf{C}, \nabla \eta) = \max_{\nabla \times \mathbf{B}} [\nabla \eta \cdot \nabla \times \mathbf{B} + h(\mathbf{C}, \nabla \times \mathbf{B})],$$

where $\nabla \eta = \rho \nabla \times \mathbf{B} - \omega \mu \mathbf{C} = \nabla \phi_R + \nabla \phi_I$ and

$$(126) \quad \tilde{h}(\mathbf{C}, \nabla \eta) = \frac{\rho}{2} |\nabla \times \nabla \times \mathbf{C}|^2 + \frac{(\omega \mu)^2}{2\rho} |\mathbf{C}|^2 + \frac{1}{2\rho} |\nabla \eta|^2 + \frac{\omega \mu}{\rho} \mathbf{C} \cdot \nabla \eta.$$

We have the following minimum variational principle

$$K = \min_{\mathbf{C}} \min_{\eta} \int_{\Omega} \tilde{h}(\mathbf{C}, \nabla \eta) d\mathbf{x} - \int_{\partial\Omega} \eta I_R ds,$$

where we impose the boundary conditions: $I_R = \mathbf{j}_R \cdot \mathbf{n} = (\mathbf{j}_R + \mathbf{j}_I) \cdot \mathbf{n} = \frac{1}{\rho} (\nabla \eta + \omega \mu \mathbf{C}) \cdot \mathbf{n}$, for $\mathbf{x} \in \partial\Omega$. Furthermore, at the minimum, the inductive reactance X' is given by

$$X' = K - \int_{\partial\Omega} [(\boldsymbol{\psi}_R + \boldsymbol{\psi}_I) \times (\nabla \phi_R + \nabla \phi_I + \omega \mu (\boldsymbol{\gamma}_R - \boldsymbol{\gamma}_I))] \cdot \mathbf{n} ds + \int_{\partial\Omega} (\phi_R + \phi_I) I_R ds.$$

Similarly, we can obtain other variational formulations of the inductive reactance, through various Legendre transformations or, equivalently, various exclusions of pairs of potentials in the system of equations

$$(127) \quad \begin{cases} \rho \nabla \times \nabla \times (\mathbf{A}_R - \mathbf{A}_I) + \omega \mu (\mathbf{A}_R + \mathbf{A}_I) = \nabla (\phi_R - \phi_I) \\ \rho \nabla \times \nabla \times (\mathbf{A}_R + \mathbf{A}_I) - \omega \mu (\mathbf{A}_R - \mathbf{A}_I) = \nabla (\phi_R + \phi_I). \end{cases}$$

All the Dirichlet type variational principles involve a double minimization over the magnetic and electric potentials. However, we observe that if instead of eliminating

pairs of potentials in (91) we exclude three potentials at once, we obtain higher order variational principles that involve a single minimization. For example, we eliminate \mathbf{A}_I , ϕ_R and ϕ_I in (91) and obtain the equation for the real magnetic field:

$$(128) \quad (\omega\mu)^2 \mathbf{H}_R + \nabla \times \rho \nabla \times \nabla \times \rho \nabla \times \mathbf{H}_R = 0,$$

with boundary conditions

$$(129) \quad \begin{cases} \mathbf{H}_R^\parallel(\mathbf{x}) = \psi_R(\mathbf{x}) \\ (\nabla \times \mathbf{H}_R)^\parallel(\mathbf{x}) = \chi_R(\mathbf{x}), \text{ for } \mathbf{x} \in \partial\Omega. \end{cases}$$

Furthermore, (128) is the Euler equation of the minimal variational formulation of the effective inductive reactance of the medium:

$$(130) \quad X = \min_{\mathbf{H}_R} \int_{\Omega} \left[\omega\mu \mathbf{H}_R \cdot \mathbf{H}_R + \frac{1}{\omega\mu} \nabla \times (\rho \nabla \times \mathbf{H}_R) \cdot \nabla \times (\rho \nabla \times \mathbf{H}_R) \right] d\mathbf{x}.$$

Similarly, the inductive reactance X is also given by

$$(131) \quad X = \min_{\mathbf{H}_I} \int_{\Omega} \left[\omega\mu \mathbf{H}_I \cdot \mathbf{H}_I + \frac{1}{\omega\mu} \nabla \times (\rho \nabla \times \mathbf{H}_I) \cdot \nabla \times (\rho \nabla \times \mathbf{H}_I) \right] d\mathbf{x},$$

where the imaginary magnetic field satisfies

$$(132) \quad \begin{aligned} (\omega\mu)^2 \mathbf{H}_I + \nabla \times \rho \nabla \times \nabla \times \rho \nabla \times \mathbf{H}_I &= 0 \text{ for } \mathbf{x} \in \Omega \\ \mathbf{H}_I^\parallel(\mathbf{x}) &= \psi_I(\mathbf{x}) \\ (\nabla \times \mathbf{H}_I)^\parallel(\mathbf{x}) &= \chi_I(\mathbf{x}), \text{ for } \mathbf{x} \in \partial\Omega. \end{aligned}$$

Finally, we derive variational principles in terms of the electric fields. We rewrite the equations (89) as

$$(133) \quad \begin{cases} \nabla \times \nabla \times \mathbf{E}_R + \omega\mu\sigma \mathbf{E}_I = 0 \\ \nabla \times \nabla \times \mathbf{E}_I - \omega\mu\sigma \mathbf{E}_R = 0, \end{cases}$$

which is the system of Euler equations associated with the min-max variational principles

$$(134) \quad R' = \min_{\mathbf{E}_R^\parallel|_{\partial\Omega}=\xi_R} \max_{\mathbf{E}_I^\parallel|_{\partial\Omega}=\xi_I} \int_{\Omega} \left[\sigma(|\mathbf{E}_R|^2 - |\mathbf{E}_I|^2) - \frac{2}{\omega\mu} \nabla \times \mathbf{E}_R \cdot \nabla \times \mathbf{E}_I \right] d\mathbf{x},$$

$$X' = - \min_{\mathbf{E}_R^\parallel|_{\partial\Omega}=\xi_R} \max_{\mathbf{E}_I^\parallel|_{\partial\Omega}=\xi_I} \int_{\Omega} \left[\frac{1}{\omega\mu} (|\nabla \times \mathbf{E}_R|^2 - |\nabla \times \mathbf{E}_I|^2) + 2\sigma \mathbf{E}_R \cdot \mathbf{E}_I \right] d\mathbf{x},$$

where we specify Dirichlet boundary conditions for the electric field \mathbf{E}^\parallel that is tangential to the surface $\partial\Omega$. The proof of (134) is very similar to the proof of Lemma 2.1, section 2.3. Next, we eliminate \mathbf{E}_I in (133):

$$(135) \quad \nabla \times \nabla \times \frac{1}{\sigma} \nabla \times \nabla \times \mathbf{E}_R + (\omega\mu)^2 \sigma \mathbf{E}_R = 0.$$

Equation (91) is the Euler equation of the variational formulation of the effective resistance of the medium, obtained by Berryman and Papanicolaou¹

$$(136) \quad R = \min_{\mathbf{E}_R} \int_{\Omega} \left(\sigma \mathbf{E}_R \cdot \mathbf{E}_R + \frac{1}{\sigma\omega^2\mu^2} \nabla \times \nabla \times \mathbf{E}_R \cdot \nabla \times \nabla \times \mathbf{E}_R \right) d\mathbf{x}.$$

¹Personal communication

The imaginary part \mathbf{E}_I of the electric field satisfies a similar variational principle

$$(137) \quad R = \min_{\mathbf{E}_I} \int_{\Omega} \left(\sigma \mathbf{E}_I \cdot \mathbf{E}_I + \frac{1}{\sigma \omega^2 \mu^2} \nabla \times \nabla \times \mathbf{E}_I \cdot \nabla \times \nabla \times \mathbf{E}_I \right) d\mathbf{x},$$

where the Euler equation $\nabla \times \nabla \times \frac{1}{\sigma} \nabla \times \nabla \times \mathbf{E}_I + (\omega \mu)^2 \sigma \mathbf{E}_I = 0$ is obtained by eliminating \mathbf{E}_R in (133). The fourth order Euler equations (like (refA52)) require the specification along the boundary of both \mathbf{E}^{\parallel} and $(\nabla \times \mathbf{E})^{\parallel}$, where the superindex \parallel denotes the components tangential to the surface $\partial\Omega$.

We conclude this appendix with the note that even though there are multiple variational formulations for the problem of quasistatic transport in conductive media, we find the saddle-point principles (25) most convenient to use in our analysis. Other variational principles of Dirichlet type are more difficult to use in the analysis because of either the higher order of the Euler equations or the nonlinearity in the high contrast function $\rho(\mathbf{x})$.

Acknowledgments. The author wishes to thank J. Berryman and G. Papanicolaou for many fruitful discussions and advice on this problem.

REFERENCES

- [1] Abramowitz, M., Stegun, I. A., 1970, *Handbook of mathematical functions*, Dover, New York.
- [2] Alumbaugh, D.L., Morrison, H. F., 1993, *Electromagnetic conductivity imaging with an iterative Born inversion*, IEEE Transactions on Geosciences and Remote Sensing, Vol. 31, No. 4, pp. 758-763.
- [3] Alumbaugh, L., Morrison, H. F., 1995, *Monitoring subsurface changes over time with cross-well electromagnetic tomography*, Geophysical Prospecting, 43, pp. 873-902.
- [4] Ambegaokar, V., Halperin, B. I., Langer, J. S., 1971, *Hopping Conductivity in Disordered Systems*, Phys. Rev. B, 4(8), pp. 2612-2620.
- [5] Batchelor, G. K., O'Brien, R. W., 1997, *Thermal or electrical conduction through a granular material*, Proc. R. Soc. London A, 355, pp. 313-333.
- [6] Bensoussan, A., Lions, J. L., Papanicolaou, G. C., 1978, *Asymptotic analysis for periodic structures*, North-Holland, Amsterdam.
- [7] Berlyand, L., Golden, K., 1994, *Exact result for the effective conductivity of a continuum percolation model*, Physical Review B (Condensed Matter), vol.50, no.4, pp. 2114-2117.
- [8] Borcea, L., Berryman, J. G., Papanicolaou G. C., 1996, *High Contrast Impedance Tomography*, Inverse Problems 12, pp. 935-958.
- [9] Borcea, L., Papanicolaou G. C., *Network approximation for transport properties of high contrast materials*, to appear in SIAM J. Appl. Math.
- [10] Cherkhev, A. V., Gibiansky, L. V., 1994, *Variational principles for complex conductivity, viscoelasticity, and similar problems in media with complex moduli*, J. Math. Phys., 35 (1), pp. 127-145.
- [11] Clerc, J.P., Giraud, G., Laugier, J.M. and Luck, J.M., 1990, *The electrical conductivity of binary disordered systems, percolation clusters, fractals and related models*, Advances in Physics, 39 (3), pp. 191-309.
- [12] Dagan, G., 1989, *Flow and Transport in Porous Formations*, Springer-Verlag.
- [13] Duvaut, G., Lions, J.L., 1976, *Inequalities in Mechanics and Physics*, Springer-Verlag.
- [14] Fannjiang, A., Papanicolaou, G., 1994, *Convection enhanced diffusion for periodic flows*, SIAM J. Appl. Math., 54, pp. 333-408.
- [15] Fannjiang, A., Papanicolaou, G., 1996, *Diffusion in turbulence*, Probability Theory and Related Fields, 105, pp. 279-334.
- [16] Fannjiang, A., Papanicolaou, G.C., 1997, *Convection enhanced diffusion for random flows*, to appear in the September issue of Journal of Statistical Physics.
- [17] Golden, K. M., *Percolation models for porous media*, in Homogenization and Porous Media, ed. Hornung, U., Springer Verlag, in press.
- [18] Halperin, B. I., 1989, *Remarks on percolation and transport in networks with a wide range of bond strengths*, Physica D, 38, pp. 179-183.
- [19] Habashy, T. M., Groom, R. W., Spies, B. R., 1993, *Beyond the Born and Rytov approximations:*

- nonlinear approach to electromagnetic scattering*, Journal of Geophysical Research, 98, No. B2, pp. 1759-1775.
- [20] Hashin, Z., Shtrikman, S., 1962, *A variational approach to the theory of the effective magnetic permeability of multiphase materials*, J. Appl. Phys. 33, pp. 3125-3131.
 - [21] Jackson, J. D., 1974, *Classical Electrodynamics*, second ed., Wiley, New York.
 - [22] Jikov, V. V., Kozlov, S. M., Oleinik, O. A., 1994, *Homogenization of Differential Operators and Integral Functionals*, Springer-Verlag.
 - [23] Keller, G. V., 1988, *Rock and Mineral Properties*, Electromagnetic Methods in Applied Geophysics, Vol. 1, Theory, (ed. Nabighian, M. N.), pp. 13-52.
 - [24] Keller, J. B., 1963, *Conductivity of a Medium Containing a Dense Array of Perfectly Conducting Spheres or Cylinders or Nonconducting Cylinders*, J. Appl. Phys., 34 (4), pp. 991-993.
 - [25] Keller, J. B., 1987, *Effective conductivity of periodic composites composed of two very unequal conductors*, J. Math. Phys., 28 (10), pp. 2516-2520.
 - [26] Kittel, C., 1966, *Introduction to Solid State Physics*, John Wiley, New York.
 - [27] Koplik, J., 1982, *Creeping flow in two-dimensional networks*, J. Fluid Mech., Vol. 119, pp. 219-247.
 - [28] Kozlov, S. M., 1989, *Geometric aspects of averaging*, Russian Math. Surveys 44:2, pp. 91-144.
 - [29] Schwartz, L. M., Banavar, J. R., Halperin, B. I., 1989, *Biased-diffusion calculations of electrical transport in inhomogeneous continuum systems*, Physical Review B, Vol. 40, 13, pp. 9155-9161.
 - [30] Shah, C. B., Yortsos, Y. C., 1996, *The permeability of strongly-disordered systems*, Physics of Fluids, vol.8, no. 1, pp. 280-282.
 - [31] Taylor, P. L., 1970, *A Quantum Approach to the Solid State*, Prentice-Hall, Englewood Cliffs, New Jersey.
 - [32] Ziman, J. M., 1971, *Principles of the Theory of Solids*, Cambridge University Press.